Sustainable Structures
ISSN: 2789-3111 (Print); ISSN: 2789-312X (Online)
http://www.sustain-dpl.com/journal/sust
DOI: 10.54113/j.sust.2025.000075

REVIEW ARTICLE

Carbonation and chloride penetration resistance of sustainable structural concrete with alkali-activated and ordinary Portland cement binders: a critical review

Osama A Mohamed[*], Haya A Zuaiter, Muhammad M. Jawa

Abu Dhabi University, Zayed City, Abu Dhabi, United Arab Emirates
[*]Corresponding Author: Osama A Mohamed. Email: osama.mohamed@adu.ac.ae

Abstract: The use of concrete with alkali-activated binders in structural engineering applications is restricted by the uncertainty surrounding its long-term performance. Durability of concrete with alkali-activated binders is particularly governed by the resistance to carbonation and chloride penetration. Carbonation lowers the pH of concrete, compromising its alkalinity, while chloride ions can induce localized corrosion of embedded steel reinforcement. This paper examines the performance of concrete where Ordinary Portland Cement (OPC) is partially or entirely substituted with supplementary cementitious materials like fly ash and ground granulated blast furnace slag (GGBS). For concrete incorporating alkali-activated binders, this review emphasizes the impact of binder composition, activator type and concentration, and curing conditions on its resistance to carbonation and chloride ingress. Methods for assessing these parameters were explored to understand the viability of alkali-activated binders in structural applications. Concrete with alkali-activated binders that contain higher calcium exhibit better resistance to chloride penetration and carbonation. Combining GGBS with fly ash enhances the carbonation resistance more effectively compared to using each binder separately to produce structural concrete.

Keywords: Sustainable concrete, alkali-activated binders, fly ash, GGBS, carbonation resistance, chloride penetration resistance

1 Introduction

Replacing a portion of Ordinary Portland Cement (OPC) with supplementary cementitious materials (SCMs) helps decrease the environmental footprint of cement manufacturing while also enhancing concrete's workability, structural integrity, and long-term durability. The amount of OPC replacement with SCMs is dependent on the chemical properties and material characteristics of the SCMs. A more sustainable and innovative approach involves the use of alkali-activation of suitable SCMs, which can completely replace OPC for the production of concrete [1]. In recent decades, significant research efforts have been dedicated to advancing sustainable alkali-activated materials (AAMs) as eco-friendly binders capable of replacing OPC. This class of AAM systems is developed through the reaction of alkaline salts, such as alkali hydroxides, silicates, with aluminosilicates such as those contained in the industrial by-products fly ash (FA) and ground granulated blast-furnace slag (GGBS) [2,3]. Despite this progress, AAMs have not been widely adopted in structural applications or engineering practices, primarily due to the limited knowledge of their long-term behavior [3–5].

Received: 1 December 2024; Received in revised form: 14 February 2025; Accepted: 2 May 2025

This article primarily examines the durability of concrete, mortar, or paste, focusing on their resistance carbonation and chloride ingress. The service life and durability of concrete exposed to carbonation and chlorides are strongly influenced by the microstructural properties of the binding gel.. The durability, along with the safety and serviceability, of reinforced concrete structures relies on the integrity of the steel reinforcing bars and their ability to resist corrosion, which is typically caused by chloride penetration or carbonation [6, 7]. Carbonation occurs when CO_2 infiltrates the concrete, lowering its alkalinity and compromising the protective oxide layer on the steel reinforcement. Similar localized depassivation of steel occurs when chloride ions reach the concrete layer in contact with the embedded reinforcement [8].

This paper examines key factors influencing carbonation and chloride ingress in concrete where the OPC binder is partially or entirely substituted with fly ash and/or GGBS, as well as the parameters that impact their performance. **Fig. 1** provides a visual representation of the most relevant keywords for this study.

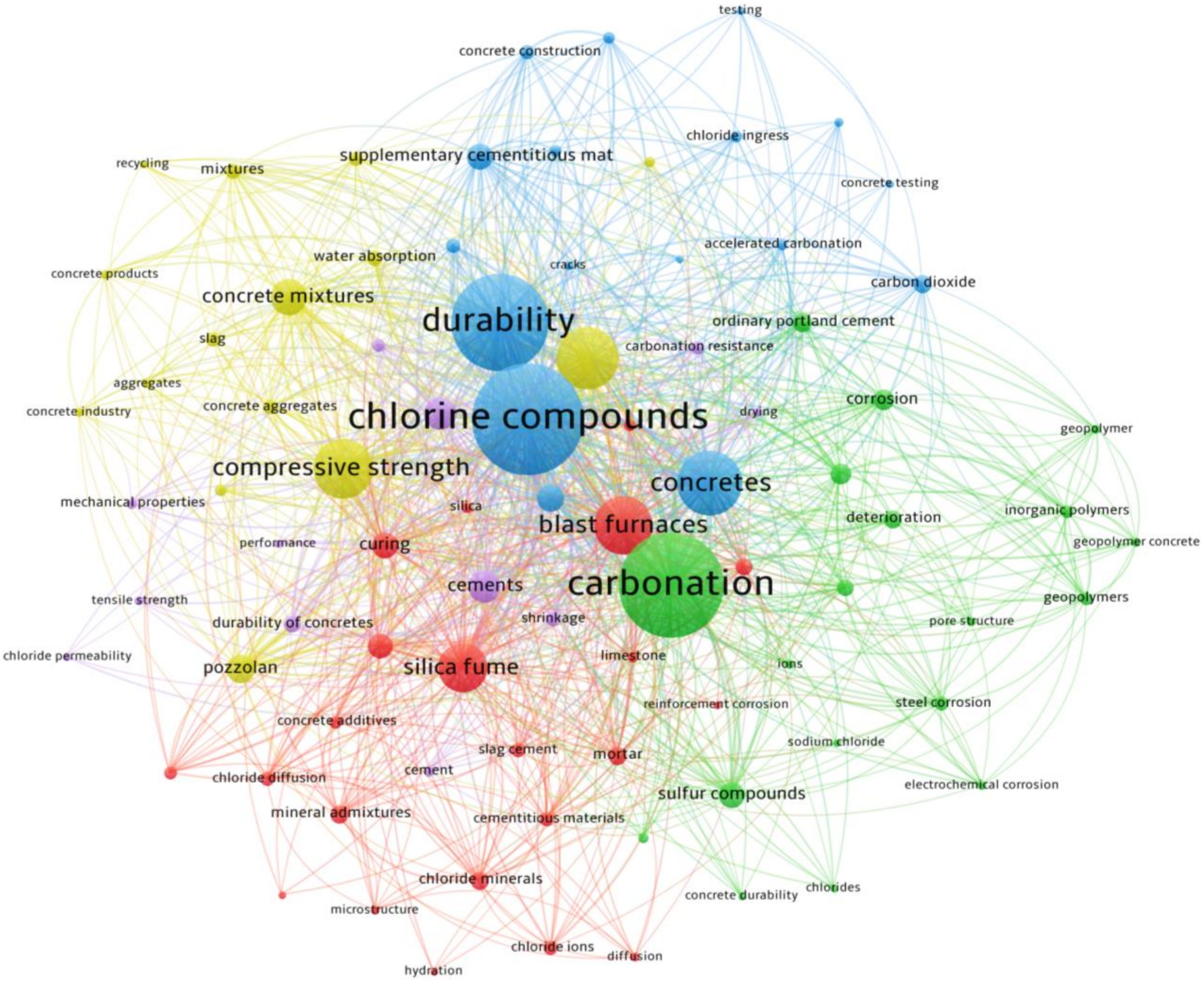

Fig. 1. Keywords covering elements of the study (VOSviewer).

2 Concrete with Alkali-activated Binders

During the manufacturing process of alkali-activated concrete (AAC), alkaline activators are essential as they initiate the necessary reactions of the binders. These activators facilitate the dissolution and subsequent polymerization of alumina and silica from the precursor materials in the alkaline solution provided by the activator, enhancing bond formation and contributing to the concrete mixture's hardening mechanism. According to the model proposed by Duxson [9] and further expanded in [10] , the reaction process in AAM unfolds in four distinct stages: dissolution, condensation, polycondensation, and ultimately, gel crystallization.

At the beginning of the reaction, aluminosilicate materials break down into reactive silicate and aluminate monomers, specifically represented as $[Si(OH)_4]^-$ and $[Al(OH)_4]^-$. A highly alkaline solution, with a pH around 14, dissolves the Si-O-Si and Al-O-Al bonds in the aluminosilicates, forming a colloidal phase. The activator solution breaks these bonds, causing insoluble particles to disperse within the mixture [9–11]. This process initiates a colloidal phase, which results in water removal through a nucleophilic substitution reaction. Negatively charged silicate (SiO_4^{4-}) and aluminate (AlO_4^{5-}) species link together through hydroxyl groups in silicates and aluminum ions in aluminates, initiating the condensation stage. This reaction generates transient compounds and reactive aluminosilicate species, along with water [9,12]. As the reaction progresses, additional water is released, leading to the formation of early-stage gels. Negatively charged silicate and aluminate species require charge-balancing alkali metal ions, such as Na^+ or K^+, to maintain stability in the alkaline solution. These ions neutralize the unstable negatively charged gels, triggering a structural rearrangement of the intermediate compounds and resulting in a more stable final material [13]. The polycondensation phase follows, resulting in the formation of stable gels throughout the geopolymeric framework and, in some cases, inducing crystallization. Some studies classify these amorphous gels as sodium-aluminosilicate-hydrate (N-A-S-H), whereas the structured phases, ranging from semi-crystalline to fully crystalline, are commonly identified as zeolites [14]. At this point, the material starts to harden, gain strength and exhibit essential characteristics typical of AAMs [11, 13].

In the context of AAMs, precursors refer to the primary raw materials that contain aluminosilicate minerals. These precursors react with alkaline activators, resulting in the development of binding phases within the final material. Typical precursor materials consist of industrial waste products like fly ash and GGBS, along with naturally occurring substances such as kaolinite or metakaolin [15, 16]. These substances provide the necessary silica and alumina that, when activated by an alkaline solution, undergo chemical transformations to form the hardened, cement-like structure of AAMs. The characteristics of concrete, mortar, and pastes made with GGBS and fly ash activated in an alkaline medium are highlighted in the subsequent sections.

2.1 Alkali Activation of Fly Ash: Effects on Microstructure and Strength of Concrete

The process of activating fly ash using alkaline materials involves an exothermic dissolution reaction [17]. During this process, the amorphous aluminosilicate network in the fly ash glass undergoes depolymerization, breaking Si–O–Al and some Si–O–Si bonds, allowing silicate and aluminate species to dissolve into the solution. Following the breakdown of the fly ash structure, there is an induction period where reaction products begin to accumulate, and little heat is released. This is followed by a strongly exothermic condensation phase, facilitating the formation of a geopolymeric matrix with an amorphous structure but high mechanical strength. The most significant factors affecting mechanical strength of alkali-activated fly ash (AAF) binders are the temperature and the type of activator used. In contrast, the activator-to-fly ash ratio exhibited a relatively lower influence on the mechanical performance [17]. In general, higher temperatures typically improve the material's mechanical strength.

Studies have shown that soluble silicates, such as sodium or potassium silicate, speed up the reaction more effectively than hydroxide activators. During these processes, the dissolution of chemical compounds, the development of hydrated and polymerized phases, and the simultaneous polycondensation of structural networks take place. Consequently, mechanical strength develops more quickly in samples activated with soluble silicates compared to those activated with hydroxides [17].

Experiments by Dhir [18] indicate that combining Class F fly ash with cement significantly reduces the porosity and permeability of the cement paste. The inherent porosity of fly-ash-based geopolymers primarily arises from the natural porous structure of the geopolymer gel. During the drying process, the loss of the aqueous pore solution results in the generation of void spaces throughout the geopolymer gel structure [19].

When Class F fly ash is activated, the resulting aluminosilicate matrix develops a mesoporous structure [20]. In pozzolanic reactions involving fly ash and calcium silicate or calcium hydroxide ($Ca(OH)_2$) present in OPC-based matrices, the initial reaction may proceed too rapidly, making it unsuitable for applications requiring extended workability or a delayed setting time. Therefore, the use of Class F fly ash is advantageous when used for concrete with OPC or as alkali-activated binder (AAB) due to its high concentration of amorphous aluminosilicates and lower content of calcium oxide. The degree of fly ash fineness is a key factor in improving the compressive strength of concrete in AAB systems. When the fly ash mean particle size is smaller than 45 µm, the compressive strength increases significantly, achieving in some cases 70 MPa within a single day [9]. Furthermore, the surface charge of fly ash particles significantly influences the early-stage reaction kinetics and setting behavior of mortar or concrete prepared using AAF binder [21].

2.2 Alkali-activated GGBS

In general, when supplementary cementitious materials (SCM) like GGBS are used to partially replace OPC, the characteristics and composition of the blended cement are highly influenced by the replacement ratio [22]. For example, substituting OPC with GGBS beyond 35% significantly lowers concrete's compressive strength at 28 days [23]. AABs have the potential to produce concrete with properties comparable to or even superior to OPC, while reducing CO_2 emissions by 80–86% [24].

Concrete developed using alkali-activated GGBS (AAS) binder faces notable challenges related to rapid setting times and poor workability [25]. These issues arise due to the amorphous structure of GGBS, along with the elevated Na_2O content in commonly used alkaline activators [26, 27]. The choice of activator significantly influences the evolution of compressive strength in AAS pastes. Pastes activated with NaOH exhibit greater early-age compressive strength than those activated using hydrous sodium metasilicate (Na_2SiO_3 $5H_2O$). However, at later stages, compressive strength increases substantially in pastes activated with sodium metasilicate compared to those activated with NaOH [28].

Puertas [29] conducted an evaluation of four different mixes with varying proportions of alkali-activated GGBS at 0 (100% OPC), 50, 70, and 90% of the total binder content. Studies indicate that GGBS-OPC blended binders generate less heat during hydration in the early stages (6 to 24 hours) while exhibiting superior compressive and flexural strength compared to pure OPC cement of the same age. This improvement was related to lower porosity and increased structural density, resulting from the development of C-A-S-H, which is tends to be more cross-linked with longer polymeric chains than the C-S-H gel present in OPC. Similarly, Bilim and Ati [30] observed that higher GGBS and sodium content in the mixture improved mechanical strength, with the peak compressive strength observed in mixes where GGBS was the sole binder. It is worth noting that after 28 days of curing, the splitting tensile strength of concrete containing 80% GGBS and 20% OPC, without an alkaline activator, was similar to that of fully OPC-based concrete [31].

Angulo-Ram ŕez [24] investigated the kinetic energy, microstructure, and the evolution of strength and durability characteristics in pastes containing a blended binder composed of 80% GGBS and 20% OPC. The results indicated that this hybrid mix, when activated with NaOH and a combination of NaOH and waterglass, exhibited compressive strengths that were 4.5 and 10.8 times higher, respectively, than those of 100% OPC. Furthermore, the hydration heat decreased, and the material exhibited a noticeably denser with more compact microstructure. Increasing the specific surface of GGBS improved the performance of the mix that used NaOH or Na_2CO_3 as activator but has the opposite effect when using $Na_2SiO_3 \cdot nH_2O$ + NaOH as activator [24]. Fernandez-Jimenez [32] reported that the durability of a mix with a binder consisting of AAS and 12% OPC is comparable to that of high-durability mix with only OPC binder. Concrete made with AAS binder achieved greater strength at 28 and 90 days than concrete with a comparable water-to-binder (w/b) ratio and OPC content [33]. With a similar binder content and w/b ratio, concrete incorporating AAS binder demonstrated reduced water absorption and capillarity compared to its OPC-based counterpart. As the GGBS content increases, both porosity and water absorption decline.

2.3 Alkali-activated Fly ash and GGBS

Despite the benefits of using alkali-activated fly ash and GGBS as binders, whether individually or in combination, there are some notable drawbacks. One significant environmental impact arises from the production of alkali activators, particularly sodium hydroxide. Additionally, these binders are prone to accelerated setting, which can lead to the formation of microcracks. If shrinkage is not adequately managed, this can result in variability in long-term strength [34]. Hence, a more innovative approach in blending alkali-activated materials to form blended or hybrid Portland cement. Blended alkali-activated binders consist of up to 30% OPC combined with substantial amounts of materials high in aluminosilicates, such as fly ash and GGBS [35–37]. Such blended cement binders with alkali activation result in hybrid cementitious materials that produce concrete and mortar with superior mechanical properties and enhanced durability, even at early stages of curing. The hydration products generated in these composites are fundamentally different in both composition and characteristics from those in conventional Portland cement. These variations primarily depend on the specific type of aluminosilicate precursor or industrial by-product utilized. Examples include Portland blast-furnace slag cement, Portland fly ash cement, and various other blended cements with components activated with alkalis [38]. These types of cements are categorized as "low carbon potential" cements.

Using either fly ash or GGBS independently as an alkali-activated binder presents certain challenges. For instance, when fly ash is utilized as the only binding material, strength development in concrete requires curing at an elevated temperature. This presents a significant challenge for its widespread application in concrete construction industry [39]. In contrast, alkali-activated GGBS can cure at ambient temperatures, but its rapid setting adversely affects concrete workability [27, 40, 41]. A promising approach for addressing these challenges involves the blended utilization of fly ash and GGBS. This blend allows for curing at ambient temperatures and mitigates the problem of fast setting, making the material more practical for industry use [42, 43]. Therefore, significant research is devoted to identifying the characteristics and long-term behavior of concrete with blended alkali-activated GGBS and fly ash (AASF) binders.

Palomo [44] investigated a hybrid binder comprised of fly ash, GGBS, and a smaller proportion of OPC (20%). The results showed that this alkali-activated hybrid binder achieved a 50% higher early-age strength, along with reduced heat of hydration and a faster setting time in contrast to similar cements lacking alkali activation. Additionally, it was confirmed that the hybrid cement forms N-A-S-H, C-A-S-H, and (N, C)-A-S-H gels during its reaction process. These findings corroborate previous studies on hybrid cements composed of 70% FA and 30% OPC [45].

The effect of AASF binders has been extensively studied, demonstrating significant impacts on the mechanical properties of the resulting materials. Flexural strength of concrete and mortar with AABs varies considerably with the composition of the alkaline activator and the type of precursor [46]. Wardhono [47] reported that AAF-based concrete exhibited an increase in flexural strength over time, whereas alkali-activated AAS-based concrete showed a decrease [27]. However, most studies reported consistent increases in compressive strength, especially for water-cured concrete. Additionally, Aiken [48] found that increasing the GGBS content in AASF concrete improved its mechanical properties and overall durability. Several studies have highlighted the effect of combining fly ash and GGBS, activated in an alkaline medium, on optimizing compressive and flexural strengths.

The type of precursor is a governing factor in the fresh properties of concrete with AASF binders [49]. In mixtures containing both GGBS and fly ash binders, GGBS-rich pastes showed a reduced slump and setting times, along with higher compressive strength relative to pastes rich in fly ash. However, the impact of the GGBS-to-fly ash proportion on compressive strength development is also governed by the NaOH concentration [50]. In addition, the environmental impact of NaOH on the global warming potential (gwp) of the concrete mix with AAS and AAF binders may be too high and nearly equivalent to using OPC as sole binder [50].

In AASF binder systems, increasing the content of GGBS decreases the pore volume [51]. At both 7-day and 28-day curing periods, neither porosity nor gel content exhibited a strong correlation with compressive strength [51]. For instance, mortar with 75% fly ash and 25% GGBS produced more gel but exhibited lower strength than its counterpart containing a greater proportion of GGBS. It is likely that concrete/mortar age, gel type and binder combination played a more significant role in strength development, especially in mortar/concrete with GGBS and fly ash binders. After a 28-day curing period, mortar with a 3:1 GGBS-to-fly ash ratio exhibited superior compressive strength compared to mixtures with both higher and lower GGBS content [51, 52]. After 7 days of curing, however, some studies reported consistently higher strength for mixes with 75%GGBS+25%fly ash [53], while others reported that mixes with 100%GGBS provide higher strength compared to others with lower GGBS content. It is hypothesized that as alkali-activated mortar/concrete matures, a blend of high content C-A-S-H and lower content of N-A-S-H is likely to provide an optimally denser and more refined microstructure that contributes most to mechanical strength, compared to even higher C-A-S-H content [52].

When the fly ash content in concrete with an AASF binder increases, particularly beyond 50%, it improves workability and enhances the quality of the finished product [54]. However, higher fly ash content adversely affects concrete strength, especially in the early ages, largely due to its slow reactivity at ambient or low temperatures. Exposing alkali-activated GGBS or fly ash concrete to high-pressure and high-temperature curing methods, such as autoclaving, significantly improves its strength development [55]. However, the inherently high early-age reactivity of GGBS makes heat curing more relevant to binders rich in fly ash. Heating increases the reaction rate and the synthesis of C-A-S-H and N-A-S-H gels in mortar/concrete with AABs. At the same higher temperature, heating accelerates the reaction of GGBS more effectively than fly ash. However, heat curing is more suitable for the precast industry than for the dominant cast-in-place applications. Prolonged curing of concrete with AAF binder produces limited enhancement in mechanical properties. However, with significant amount GGBS (≥ 50) prolonged curing at ambient temperatures produces concrete with significant improvements in mechanical properties. Similarly, if a small amount of GGBS ($\leq 25\%$) is blended with fly ash, heating is typically necessary to attain competitive mechanical properties.

Beyond typical curing periods, sustained exposure to elevated temperatures for prolonged periods has complex effects on microstructure and mechanical properties. Ma [56] demonstrated that curing at 60 ℃ for 3 days enhances the strength of mortar containing blended AASF binders. Sustained exposure to the same temperature for 28 days enhances compressive strength, mainly as a result of the extended mean chain length (MCL) in the gel structure. A longer MCL of C-A-S-H and/or N-A-S-H gel is associated with a more interconnected network and a denser, more compact gel, leading to enhanced mortar strength [53]. Sustained exposure to the same temperature for 28 days enhances mechanical strength, mainly due to the extended mean chain length (MCL) in the gel structure, which contributes to a denser and more cohesive matrix [56]. However, if the exposure temperature is much higher, e.g. 800 ^{0}C, the duration that leads to microstructural changes including increase in cracking and porosity of mortar with GGBS/fly ash binder can be as short as 120 minutes [57]. When fly ash: GGBS ratio is 4:1, heating to 400 ^{0}C produces Al/Si ratio between 0.36 and 0.46, which classifies the gel as silica-rich N-A-S-H, while heating from 400 ^{0}C to 800 ^{0}C increases the Al/Si ratio from 0.4 to 0.79, which identifies N-A-S-H as Al-rich [57]. As experimental test temperature was elevated from 200 ℃ to 800 ℃, the Ca/Si ratio in AASF mortar decreased from 0.68 to 0.55, signifying the decomposition of C-A-S-H gel under intense heat.

3 Carbonation of Concrete with Alkali-activated Binders

Carbonation occurs when ambient CO_2 diffuses into the concrete matrix and reacts with $Ca(OH)_2$, leading to the formation of calcium carbonate ($CaCO_3$) as a solid. This reaction decreases concrete alkalinity, which can compromise the protective oxide film surrounding the embedded reinforcing steel bars, increasing the risk of corrosion and potentially diminishing the structure's long-term durability [58, 59].

In concrete with AASF binders, the carbonation process differs slightly from that of traditional Portland cement concrete. For these AAMs, CO_2 reacts with the AAB network, resulting in the development of carbonate phases like calcium and sodium carbonate. These compounds can impact the strength, structural integrity, and durability of the concrete [60].

The understanding of carbonation in AAMs is less clear compared to OPC-based compounds, though their carbonation mechanisms share fundamental similarities. AAMs with higher calcium content exhibit better resistance to carbonation, higher CO_2 absorption, and improved performance [61]. For AAMs with comparable microstructures and porosity, carbonation behavior differs based on the chemical makeup of the precursor. This variation influences properties like pore distribution, dimensional stability, durability, and strength [62]. Apart from the inherent characteristics of the materials, especially porosity, key factors influencing carbonation include the choice of precursor, the alkali activator’s reactivity, pre-exposure curing conditions, and the parameters of the accelerated carbonation environment [63, 64].

Research indicates that a higher GGBS content and sodium concentration in the mixture enhance both flexural and compressive strengths of concrete. However, these alkali-activated materials are more sensitive to carbonation than traditional OPC-based mortars due to greater CO_2 penetration.

3.1 Effect of Binder Type

3.1.1 Carbonation Behavior of Concrete and Mortar with Fly Ash Binder Activated in an Alkaline Medium

Badar [65] studied the carbonation behavior of concrete with an AAF binder by evaluating three fly ash variants with different calcium oxide (CaO) contents. After up to 450 days of exposure to carbonation, all samples exhibited higher porosity, a reduced pore solution pH, and a decline in compressive strength. While the exact carbonation mechanism remained unclear, the formation of sodium carbonates from CO_2 was identified as the main factor contributing to pore network degradation and structural weakening [65]. Bernal [62] observed that the presence of magnesium oxide (MgO) in GGBS mitigates early-age carbonation deterioration (within 14 days). This protective effect is primarily ascribed to the development of additional phases, including layered double hydroxides (LDHs), which form through the direct uptake of CO_2. LDHs enhance the durability of concrete through pore-filling, leading to a more stable structure.

The carbonation depth in pastes with AAF binders is a function of the duration of CO_2 exposure [66, 67], as illustrated in **Fig. 2** [67]. You [68] observed that extending the exposure to carbonation from 28 to 56 days led to a greater carbonation depth in alkali-activated specimens. For specimens containing 20% fly ash (FA) and 80% phosphorous GGBS (P), the carbonation depth rose from 5.2 mm to 5.85 mm. Phosphorous GGBS has high levels of phosphorus content that delays the setting time.

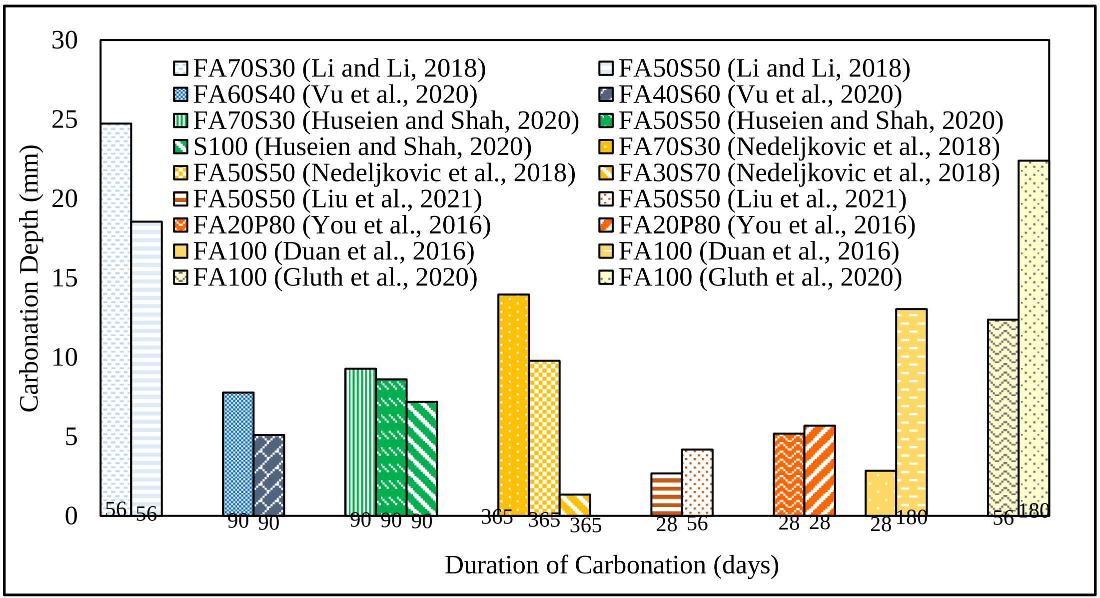

Fig. 2. Carbonation depth of AASF binders (FA= fly ash; S=GGBS) [67].

Fly ash-based geopolymer samples containing 10% GGBS exhibited a notable increase in carbonation depth as CO_2 concentration rose from 1% to 3%, when cured at 23 ℃ and 55% relative humidity (RH). [69]. When GGBS partially replaced fly ash at levels of 30%, 50%, and 70%, the extent of carbonation was reduced by 43.6%, 67.27%, and 92.72%, respectively, in comparison to specimens made entirely of fly ash. These tests were conducted in a controlled indoor laboratory environment at 20 ℃ and 55% RH [70]. This suggests that incorporating GGBS into alkali-activated concrete (AAC) made with fly ash enhances its carbonation resistance compared to using fly ash as only binder. The greater carbonation depth observed with increasing fly ash content was linked to the inherently lower CaO levels, changes in the binder's chemistry, and modifications in pore structure that led to increased porosity [71, 72]. In the initial stages, the significant increase in carbonation is due to the sluggish pozzolanic activity of fly ash, which slows the development of reaction products and impedes matrix densification. The slow development of polymerization products causes higher porosity and higher penetration of CO_2 through concrete with fly ash-based binder.

3.1.2 Carbonation of Alkali-activated GGBS

Several studies have indicated that the deterioration mechanism of carbonated mortar with an AAS binder involves decalcification of the C-S-H gel [37, 73]. GGBS binders activated with sodium silicate produce fewer carbonation byproducts than those activated with NaOH, leading to reduced mechanical strength and higher porosity following carbonation. Conversely, in NaOH-activated GGBS mortars, carbonation compacts the binding matrix leading to improvement in mechanical strength [37].

GGBS activated with sodium silicate is more prone to carbonation due to its lower calcium-to-silicon (Ca/Si) ratios. This increased susceptibility arises because the limited calcium ions (Ca^{2+}) in the C-S-H gels are converted to calcium carbonate ($CaCO_3$) in a low-pH environment during carbonation [73]. Consequently, this transformation results in a significant reduction in binding strength due to the increased susceptibility of C-S-H gels to decalcification [73]. **Fig. 3.** shows that carbonation of mortar with OPC binder increases compressive strength while it has the opposite effect when the binder is GGBS activated with waterglass moduli ranging from 0 to 1.5. One justification for the strength degradation of mortar with GGBS binder is the decalcification of the C-S-H gel.

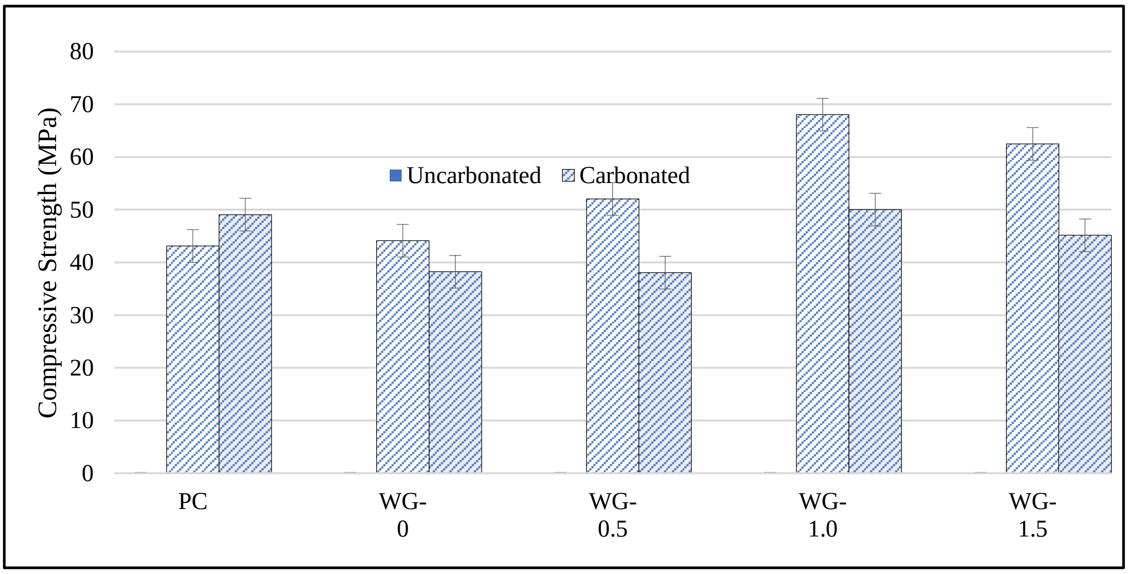

Fig. 3. Influence of carbonation on compressive strength of mortar with OPC and AAS binders with various water glass (WG) moduli from 0 to 1.5 (WG-0 to WG-1.5) [73].

It was reported that adding metakaolin (MK) affects CO_2 diffusion and increases carbonation depth in mortar with AAS binder [74]. This is due to the lower levels of CaO and MgO in MK compared to GGBS. Samples without MK exhibited greater trona phase formation during carbonation, indicating a higher availability of unbound Na^+ ions in the pore solution [74]. In contrast, metakaolin-blended specimens saw the development of aluminosilicate gel, which helped bind Na^+ ions.

Alkali-activated GGBS with higher MgO content produces concrete/mortar with higher carbonation resistance. Reactive MgO undergoes hydration, resulting in the formation of $Mg(OH)_2$, which subsequently reacts with CO_2 to produce $MgCO_3$ [62]. Studies also identified the existence of Mg-Al hydrotalcite phases forming during carbonation. Therefore, the resistance to carbonation exhibited by concrete with AAS binder depends not only on the content of CaO, but also on the presence of other uncarbonated alkaline-earth metal components [62].

For concrete with an AAS binder, as with AAF, prolonged exposure to CO_2 results in deeper carbonation penetration. Although studies comparing the rate of carbonation progression in OPC-based concrete and those with blended GGBS-fly ash alkali-activated binders are limited, it is evident that they generally exhibit this trend. According to data reported by Bernal [33], increasing the GGBS content from 300 to 500 kg/m ^{3}significantly enhanced the mortar's ability to resist carbonation. The mix with the least GGBS exhibited the highest carbonation depth, with approximately 70% of the specimen undergoing carbonation. Therefore, the binder content significantly influences the resistance to carbonation exhibited by mortar with an AAS binder.

3.1.3 Carbonation of Concrete with Combined Fly ash and GGBS Binders

As discussed earlier, alkali-activated GGBS binder produced concrete/mortar with improved carbonation durability relative to fly ash-based mixtures. Replacing fly ash with GGBS at proportions of 30%, 50%, and 70% led to substantial reductions in carbonation depth, quantified as 43.6%, 67.27%, and 92.72%, respectively, compared to samples made solely with fly ash, under controlled indoor conditions (20 ℃ and 55% RH) [70]. These findings highlight that partial replacement of fly ash-based binders with GGBS enhances carbonation resistance of concrete compared to using fly ash as sole binder. As mentioned previously, the greater carbonation depth observed with higher fly ash content was linked to a decrease in CaO levels and changes in the pore structure, resulting in increased porosity [71].

Further research has explored the influence of CO_2 exposure duration on the carbonation penetration depth of concrete with AABs. For instance, extending the carbonation duration from 28 to 56 days led to a greater carbonation depth, increasing from 5.2 to 5.85 mm in samples containing 20% fly ash and 80% phosphorus GGBS [68]. Similarly, increasing the CO_2 concentration from 1% to 3% significantly increased the carbonation depth in geopolymer specimens with a primarily AAF binder containing 10% GGBS, cured at 55% relative humidity and 23 ℃ [69].

In mortar with AAF binder, the level of fly ash substitution with GGBS significantly influences the evolution of pore structure. Nedeljković [75] reported that in pastes with high GGBS content, porosity was markedly reduced to approximately 4% when the GGGBS content reached 100%. Higher GGBS content led to a refinement in the pore size distribution along with decrease in permeability and a slowing down in diffusion of CO_2 through the paste [75]. **Fig. 4** shows that the carbonation coefficient (mm/day$^{0.5}$) decreases as the relative content of GGBS increases. The figure also shows sealed paste samples exhibited lower carbonation coefficient compared to unsealed ones.

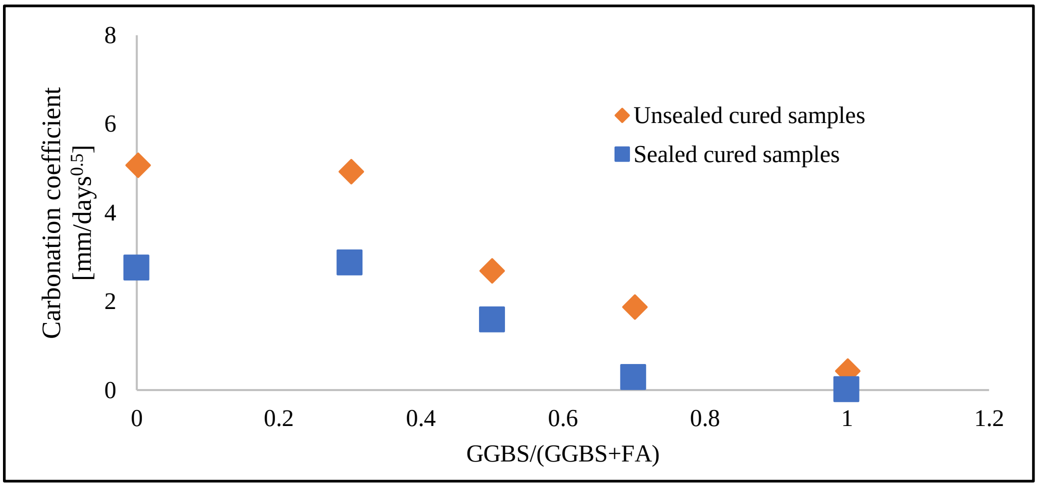

Fig. 4. Effect of GGBS content with respect to total GGBS+fly ash binder and curing on carbonation coefficient [75].

The addition of reactive MgO in OPC-based concrete generally enhances mechanical properties, including stiffness elastic modulus, compressive strength, and toughness [76]. During the carbonation process, reactive MgO captures and chemically binds CO_2, forming carbonate phases. This reaction decreases the amount of CO_2 available for interactions with other components, potentially slowing down the overall carbonation rate. However, there is limited research available on the carbonation mechanism or the impact of reactive MgO on modifying carbonation behavior in AASF binders [77].

Wang [78] examined the influence of reactive magnesium oxide (MgO) on the carbonation behavior of mortar with an AASF binder aged for 90 days. The research observed a substantial increase in compressive strength across all samples after a 28-day carbonation period and identified aragonite as the primary carbonation product. While compressive strength showed only slight variations between 28 and 90 days, samples with a higher reactive MgO content exhibited notable strength increases, reaching up to 74.8% post-carbonation [78].

3.2 Effect of Activator Type and Concentration on Carbonation Resistance

The performance and service life of alkali-activated concrete (AAC), particularly in terms of carbonation, are significantly influenced by the concentration as well as the type of the activator. The extent of carbonation in AAMs is determined by the concentration of CO_2 and its diffusion through the specimen, both of which are heavily influenced by the material's porosity. Porosity is ultimately governed by the composition and molarity of the alkali activator. Alkaline activators are known to induce rapid hardening and enhance compressive strength. Wang and Scrivener [79] indicated that the primary reaction product when AAS is activator is C-S-H with low Ca/Si ratio, regardless of the activator used. Among the factors influencing the development of mechanical strengths in AAMs, the type of alkaline activator has the most significant impact, followed by activator concentration, curing temperature, and the specific surface area of the material [80].

Several studies investigated the microstructural changes in mortar developed using GGBS activated with NaOH and sodium silicate solutions [81, 82]. Increasing the Na_2O content and the SiO_2/Na_2O ratio in the activator significantly enhanced the resistance to carbonation. The enhanced performance was linked to a reduction in the overall porosity and the average pore size of the hardened material. Likewise, an experimental study on hybrid cements, comprising 80% GGBS and alkali-activated with NaOH and Na_2SiO_3 solutions, demonstrated that both the activator type and its concentration significantly influence the formation of the resulting phases and strength characteristics [24].

Tests by Li [73] indicate that mortars with a GGBS binder activated solely with NaOH demonstrated superior carbonation resistance, as reflected in their greater residual strength, in contrast to those activated using a mixture of Na_2SiO_3 and NaOH. Raising the SiO_2/Na_2O ratio in the activator produced C-S-H with a reduced Ca/Si ratio, which accelerated the decalcification process due to the lower availability of calcium hydroxide (CH).

Avila [83] assessed the mechanical properties of AAM made from municipal incinerator bottom ash (MIBA) and fly ash (FA) with varying proportions of NaOH and Na_2SiO_3 under forced carbonation. The results demonstrated that changes in the Na_2O/binder and SiO_2/Na_2O ratios influenced the porosity profile of the hardened specimens with fly ash binder activated using NaOH and Na_2SiO_3, thereby affecting their carbonation resistance. This was evident from the different compressive strengths observed in carbonated fly ash and MIBA samples under varying alkaline solution compositions.

The influence of different activator combinations on the microstructural and mechanical properties of mortar with an electric arc furnace slag (EAFS) binder was investigated by Kassim [84]. The authors focused on the different combinations of NaOH and Na_2SiO_3 on EAFS mortars under forced carbonation. The study and several others consistently found that increasing the Na_2O/binder and SiO_2/Na_2O ratios led to a more compact microstructure with lower porosity, enhancing the mechanical strength and carbonation resistance of the specimens [73, 83]. Typically, an optimum alkali activator content exist that maximizes the performance, exhibits decreased porosity, and reduces CO_2 diffusion. However, when considering CO_2 uptake, the optimal values for Na_2O content and SiO_2/Na_2O ratio differ between uncarbonated and carbonated specimens. **Fig. 5** shows that 28 day accelerated carbonation curing of EAFS mortar with 6% Na_2O concentration increases compressive strength relative to similar samples without carbonation curing. The increase in strength is also dependent on the silicate modulus ($S= SiO_2/Na_2O$).

The amount of Na_2O in the activator influences the amount of C-A-S-H produced during activation of GGBS. A rise in Na_2O content of the activator from 4% to 8% results in greater C-A-S-H gel production. C-A-S-H gel increases the amount of calcium carbonate in the binder. Similarly, in AAF binders, a higher Na_2O content accelerates the reaction rate, enhancing N-A-S-H gel development, which in turn decreases the carbonation rate in mortar [85].

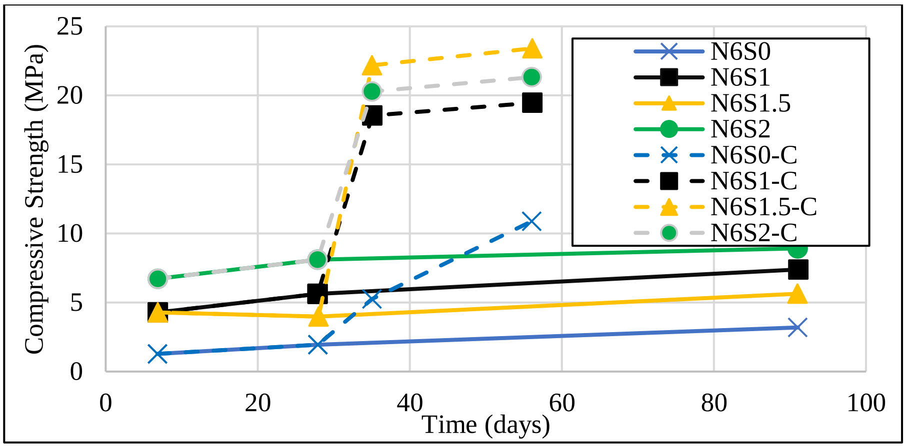

Fig. 5. Average compressive strength of EAFS mortar with 6% Na_2O (N6) concentration, varying silicate moduli (S= SiO_2/Na_2O = 0, 1.0 to 2) and curing with carbonation (letter C) and without carbonation [84].

3.3 Impact of Curing Conditions on Microstructure, Strength, and Carbonation of Mortar and Concrete

The curing conditions of AAMs significantly impact their carbonation behavior. Various AABs have unique chemical compositions and undergo different reactions [15]. The influence of the curing environment and the content of GGBS on gel formation in AASF pastes was studied by various researchers [75]. When subjected to carbonation, the curing conditions of alkali-activated pastes/mortar significantly affect the phase chemistry and microstructural evolution of the material. The effect of curing became particularly prominent after 28 days, whereas no significant differences were observed between sealed and unsealed pastes after just 7 days. The variation in composition is due to the loss of Na^+ ions in unsealed samples, which led to the development of Ca-Al-Si-H gel instead of Ca-Na-Al-Si-H [75]. Conversely, sealed samples retained higher Na+ content in the Ca-Na-Al-Si-H gel. The effect of curing environment on chemical composition and proportions of the gel phases was more pronounced in pastes with 50% GGBS compared to those with 100% GGBS.

Nedeljković [75] examined CO_2 penetration in alkali-activated concrete (AAC) produced using a blend of fly ash and GGBS, subjected to various curing conditions, including wet, dry, and CO_2 curing. In the wet curing phase, some specimens were sealed while others remained exposed, whereas during dry and CO_2 curing, all samples were unsealed. The findings revealed that CO_2 diffusion occurred more rapidly in unsealed specimens, likely due to microstructural changes resulting from Na^+ ion dissolution and migration, which led to higher interconnected porosity and increased carbonation depth. Specimens containing GGBS exhibited significantly lower carbonation depths and greater resistance to carbonation than their fly ash-based counterparts, regardless of the curing method. This improved resistance was attributed to the greater CaO content in GGBS, which helps maintain pore solution pH and slows carbonation progression.

Morone [86] investigated the behavior of AAMs with a Basic Oxygen Furnace (BOF) slag binder, analyzing the influence of varying curing temperatures on carbonation kinetics and material performance. BOF slag samples were synthesized with varying types and molarities of alkali activators and under different curing environments. These conditions included curing for 3, 7, and 28 days, at 20 ℃, 22 ℃, and 50 ℃, relative humidities of 75% and 98%, and a CO_2 concentration of 5%. The research revealed that samples cured and carbonated at 50 ℃ exhibited a consistent carbonation progression over time, irrespective of other controlled variables [86]. This phenomenon was attributed to the early development of a carbonate layer on the exterior of the samples, which effectively blocked further CO_2 diffusion.

Fig. 6 illustrates that curing mortar with a Basic Oxygen Furnace (BOF) slag binder, activated by NaOH and Na_2SiO_3, in a carbonation chamber at 50 ℃ enhances compressive strength relative to samples cured at lower temperatures or those activated with a blend of NaOH and Na_2CO_3 [86].

Higher curing temperatures of alkali-activated GGBS mortars enhance early-age mechanical strengths when sodium silicate hydrate ($Na_2SiO_3 \cdot nH_2O$) and sodium hydroxide (NaOH) or sodium carbonate (Na_2CO_3) are used as activators [80]. However, elevated curing temperatures do not contribute to improvements in mechanical strength at later ages. Behfarnia and Rostami [87] evaluated the carbonation of alkali-activated GGBS samples cured under water compared to samples cured under plastic film. The alkali-activated GGBS binder was partially replaced with 5% to 15% microsilica (95–85% GGBS), and the samples were exposed to approximately 4% CO_2 for 28 days. The samples with alkali-activated GGBS binders that were cured in water showed lower carbonation depths and enhanced compressive strengths than those cured under plastic sheets, indicating the effectiveness of water-based curing in reducing carbonation. The positive effect of water curing on enhancing the compressive strength of mortar with AAS and AAF binders has been confirmed by other researchers [88].

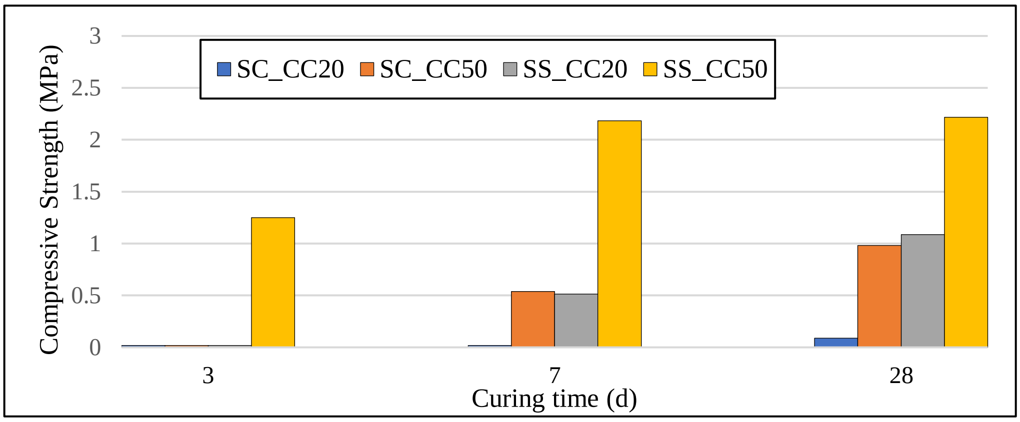

Fig. 6. Compressive strength of mortar with NaOH + Na_2CO_3 (SC), NaOH+Na_2SiO_3 (SS) activators, cured in carbonation chamber (CC) at 20 ^{0}C (CC20 or 50 ^{0}C (CC50) [86].

Given that carbonation in AAC is largely dependent on its microstructure, suitable curing conditions can promote a denser, more homogeneous matrix with enhanced carbonation resistance. The best results are typically achieved by minimizing excessive moisture exchange with the surroundings. Methods such as sealed curing or maintaining a moderately humid environment (without full saturation) are considered most effective. In contrast, curing in a dry environment can cause significant water loss, reducing the development of C-(N-)A-S-H gels, while direct water contact can lead to the dissolution of soluble Na, resulting in leaching and degradation of the microstructure [15]. In fact, it was argued that immersion of mortar with AABs in solution, including acids, retains reactants with the sample which facilitates continuity of the geopolymerization process and continued enhancement in mechanical properties [50, 88].

3.3.1 Accelerated Carbonation Curing

Early-age curing by exposing concrete to concentrated CO_2 in a controlled environment has emerged as a promising method for enhancing CO_2 sequestration and reducing the carbon footprint of the concrete industry [89]. The process involves capturing and storing CO_2, then reusing it in a controlled environment for concrete curing, which enhances the durability and strength of OPC-based materials. The need for a controlled curing environment and closed chambers makes the method particularly more suitable for precast concrete products [90].

Increasing CO_2 partial pressure from 0.1 to 10 bars has been found to accelerate the carbonation process, enhancing CO_2 absorption and improving durability and strength of OPC-based concrete [60]. Alkali-activated GGBS concrete achieved peak CO_2 uptake of 12.8% by mass of binder after 4 hours of preliminary curing, then subjected to 20 hours of carbonation treatment under 5 bars of pressure. Extending both the initial and carbonation curing periods, combined with increased pressure, led to enhanced compressive strength and lower water absorption. Additionally, carbonation curing reduced the carbon footprint of concrete that used AAS binder by up to 46% compared to its non-carbonation-cured counterparts. Carbonation curing of geopolymer concrete and mortar is a promising alternative to further lower the environmental impact of cement production while recycling industrial byproducts [15].

Wardhono [47] observed that after carbonation, the pH of concrete that is based on fly ash binder ranged from 11 to 12, while OPC-based concrete displayed a broader pH range of 9 to 13. Other research indicated that the pH of concrete developed using AASF binders remained above 10.2 when measured at the steel reinforcement level, suggesting its suitability for reinforced concrete structures, as steel corrosion typically begins when the pH drops below 10.0 [91].

CO_2 concentration, relative humidity, pressure, and temperature are key factors that affect the carbonation process and alter the microstructure of alkali-activated concrete [15]. In experimental carbonation studies, relative humidity is maintained at around 60%, as this level promotes significant carbonation, at a rate comparable to that in OPC concrete. While higher CO_2 concentration and partial pressure generally correlate with greater carbonation depths, excessively high CO_2 levels can lead to increased acidity, potentially dissolving calcium carbonate and altering the carbonation process. This issue can be mitigated by carefully controlling the relative humidity to ensure the oversaturation of Ca^{2+} in the acidic solution, causing a spontaneous precipitation of carbonate compounds. Table 1 shows a summary of studies on the effect of concrete and mortar with AABs as well as OPC.

Table 1. Summary of studies carbonation resistance of concrete with alkali-activated and OPC binders (CR: Carbonation Resistance; CST: Compressive Strength; CD: Carbonation Depth; CRA: Carbonation Rate).

Parameter	Binder and Activator	Carbonation Conditions	Conclusion
CR [37]	Binder: 100% GGBS Activators: (1) NaOH (2) Waterglass	CO_2-saturated, 43.2% RH	Compressive strength increases when NaOH is used as a GGBS activator, as the precipitation of $CaCO_3$ within the pores reduces overall porosity. Waterglass induces gel decalcification during carbonation, leading to strength degradation.
CR [92]	Binder: Fly ash Activator: Na_2SiO_3 + NaOH	20 ± 3 % CO_2, 20 ± 2 ℃, 70 ± 5 % RH	Mechanical strength of concrete with activated fly ash binders remain stable, while OPC-based concrete exhibits increased brittleness after carbonation.
CST [74]	Binder: GGBS Activator: Na_2SiO_3 + NaOH	3.0 ± 0.2% CO_2, 20 ± 2 ℃, 65 ± 5% RH	The compressive strength of GGBS-based mortar was 63 MPa after 28 days. Exposure to 3% CO2 led to a significant reduction in strength, between 40-50%.
CR [93]	Binder: Fly ash + GGBS Activator: NaOH + KOH	Natural carbonation	High levels of GGBS in alkali-activated systems reduce both the average pore size and porosity, which decreases the diffusion of CO_2 into concrete.
CR [94]	Binder: GGBS Activator: Waterglass	Natural carbonation	GGBS-based binders activated with waterglass exhibit better carbonation resistance due to their smaller average pore sizes and lower total porosity.
CD [95]	Binder: GGBS Activator: Na_2SiO_3 + NaOH	10–20% CO_2, 70% RH.	GGBS-based concrete experienced greater strength loss and deeper carbonation depths compared to OPC concrete when subjected to 0.352M Na_2SiO_3 solution and 10-20% CO_2.
CD [96]	Binder: GGBS Activator: Waterglass Water to binder ratio: 0.42, 0.48	Natural carbonation	The carbonation depths of concrete with sodium silicate-activated GGBS binder and w/b ratios of 0.42 and 0.48 were similar after seven years of exposure to CO_2. The binder composition and pore volume had a more substantial effect on resistance to carbonation than the w/b ratio.

CRA and CD [69]	Binder: Fly ash + GGBS Activator: Na_2SiO_3 + NaOH	3% CO_2, 23 ℃, 55% RH	Different CO_2 concentrations produce varying carbonation products. As CO_2 concentration increases, the carbonation rate and depth in concrete increase.
CRA [97]	GGBS Activator Na_2SiO_3 + NaOH	(1) Natural carbonation (2) 1% CO2, 19 to 38 ℃, 70 and 76% RH	Under natural carbonation conditions (19-38 ℃ and 70-76% relative humidity), GGBS-based concrete showed lower carbonation depths compared to those predicted under accelerated carbonation conditions (1% CO_2).
CR [98]	Cement	Natural carbonation	Binders with a Ca/Si ratio below 0.66 experience extensive decalcification, leading to the breakdown of calcium oxide sheets and high shrinkage due to calcium carbonate precipitation.
CR [99]	GGBS Activator: (1) Carbonate (2) Carbonate +Hydroxide	Natural carbonation	GGBS activated with carbonates or a mix of carbonates and hydroxides demonstrated high stability under natural carbonation conditions, showing an acceptable carbonation rate after 35 years of exposure.
CR [100]	GGBS Activator: Na_2SiO_3 + NaOH	1% CO_2, 60% RH	The carbonation of GGBS powdered pastes results in gel decomposition and calcium carbonate formation, with most CO_2 diffusion occurring within the first 28 days.
CR [8]	Fly ash + GGBS Activator: Na_2SiO_3 + NaOH	1–5% CO_2, 23 ± 2 ℃, 65% RH.	The N-A-S-H gel remains largely unaffected, whereas the C-A-S-H gel loses calcium and transforms into cross-linked residual silicate gel. Fly ash-based binders primarily carbonate by forming bicarbonate salts in the pore solution.
CRA [101]	Fly ash + GGBS Activator: Na_2SiO_3 + NaOH	5% CO_2, 20 ℃, 60% RH	The carbonation rate decreases as the GGBS ratio in active fillers increases, with finer GGBS particles further reducing the carbonation rate coefficient.
CR [65]	Fly ash (with different CaO contents) Activator: Na_2SiO_3 + NaOH	5% CO_2, 24 ± 5 ℃, 65 % RH	Accelerated carbonation testing on fly ash-based binders results in a reduction in pH, decreased strength, and increased total porosity.
Calcium carbonate content [85]	GGBS + Fly ash Activator: Na_2SiO_3 + NaOH	1.0 ± 0.2% CO_2, 20 ± 2 ºC, and 65 ± 2% RH	Mortars activated with both sodium hydroxide and sodium silicate showed better carbonation resistance compared to those activated with sodium hydroxide alone.
CR [75]	GGBS + Fly ash Activator: Na_2SiO_3 + NaOH	0.04% CO_2, 20 ℃, 99% RH	Sealed curing at high relative humidity improved the carbonation resistance of pastes with alkali-activated fly ash/GGBS binders by preventing alkali leaching and maintaining alkalinity.
CRA [8]	GGBS Activator Na_2SiO_3 + NaOH	1.0, 3.0, 5.0 ± 0.2% CO_2, 23 ± 2 ℃, 65 ± 5% RH	Carbonation rate of GGBS-based concretes is affected by CO_2 concentration. Higher CO_2 concentrations result in significant changes to total porosity.
CR [102]	Binder: GGBS Activator: Na_2SiO3 + NaOH	Natural carbonation	GGBS-based concrete with a strength of 30 MPa showed a high carbonation rate, while concrete with strengths between 30 MPa and 50 MPa had a medium rate. Concrete with strengths above 50 MPa exhibited carbonation rates similar to OPC concrete.

4 Chloride Penetration in Concrete with Alkali-activated Binders

Chloride ions, commonly introduced from materials like sea sand or exposure to marine environments, can penetrate the concrete's porous structure through absorption, wicking, and diffusion. Absorption occurs due to capillary forces that draw chloride ions inward, while wicking is influenced by hydrostatic pressure, pushing these ions into the cement matrix through surface pressure differences. [103]. Diffusion, on the other hand, results from variations in concentration between the external and internal environments.

In AAMs, chloride transport is heavily affected by the characteristics of the hardened matrix, including composition of pore solution, overall porosity, tortuosity, pore size distribution, and the material's chloride-binding capacity. Research has shown that parameters such as precursor physicochemical properties, activator composition, and curing regimes play a crucial role in modifying porosity and pore structure, ultimately influencing chloride ingress [104–106].

The deterioration of steel reinforcement, primarily driven by chloride ion ingress due to contact with de-icing salts, marine or similarly harsh environment, poses a significant risk to the durability and load-carrying capacity of reinforced concrete systems [48]. When the chloride level at the steel surface exceeds its critical concentration, the passive layer breaks down, triggering corrosion [107]. Therefore, understanding the chloride resistance of concrete developed using AABs is essential to promote their use in reinforced concrete.

4.1 Effect of Binder Type

4.1.1 Chloride Resistance of Mortar and Concrete with Fly ash Binder Activated in Alkaline Medium

Variations in particle geometry and liquid demand among fly ashes from different sources can greatly influence the pore structure of the hardened material [108]. Coarser fly ash generally requires an increased amount of water to achieve the desired workability, which in turn necessitates a larger amount of activator, resulting in higher porosity and permeability [46]. Consequently, neat fly ash mixes have been shown to exhibit poor resistance to chloride penetration [48]. This increased porosity raises concerns about the durability of AAF-based concrete, as sulphate and chloride ions can infiltrate the structure and potentially compromise the reinforcement [108].

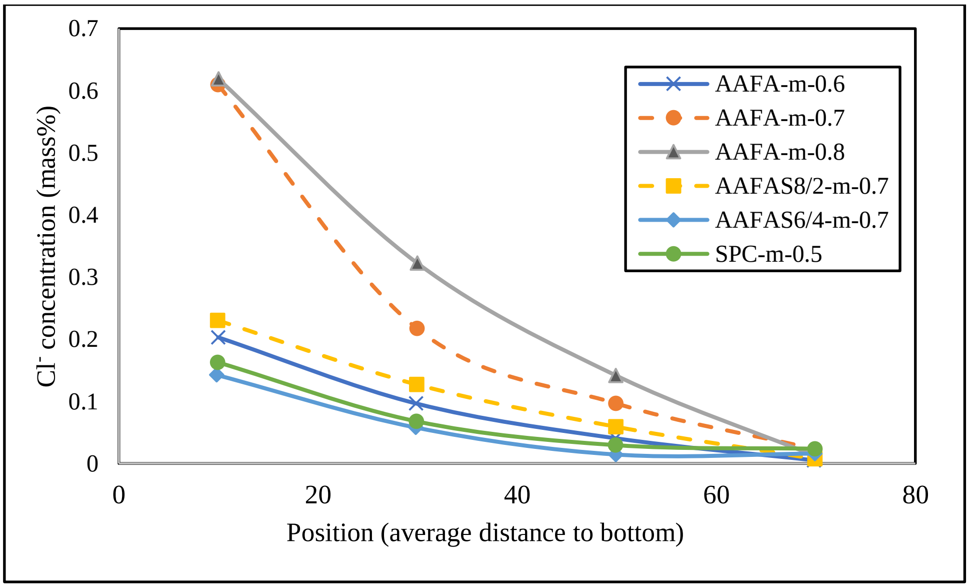

Fig. 7. Penetration of chloride ions through mortar (m) with AAF binder at different liquid/solid ratios (0.6, 0.7, and 0.8) and 20% or 40% slag replacement (AAFAS8/2 and AAFAS6/4) [108].

Zhu [108] reported that unsaturated mortar with AAF binder may have higher chloride penetration rates than the OPC-based counterparts. The chloride penetration rate is impacted by the material’s tortuosity and porosity, which, in turn, are affected by the liquid-to-solid (L/S) ratio and the degree of fly ash substitution with GGBS, if applicable. Lowering the L/S ratio from 0.8 to 0.6 reduces the porosity of AAF paste from 42.2% to 37.0%, which in turn decreases chloride ingress by 40–60%. Substituting 20–40% of fly ash with GGBS at the same L/S ratio of 0.7 does not significantly alter porosity but decreases pore sizes and increases matrix tortuosity, both of which help lower chloride penetration rates.

Fig. 7 depicts the impact of an L/S ratio increase from 0.6 to 0.8, which led to higher chloride ion penetration in mortar with an AAF binder. Similarly, replacing fly ash with 20% and 40% slag binder decreases the penetration of chloride ions through mortar substantially [108].

Olivia [109] reported that concrete with an AAF binder exhibited higher chloride ion penetration than its OPC-based counterparts. There is, however, a significant variability in the relative chloride penetration resistance across different studies, which underscore the need for further research into the durability performance of AAFA mixes [110]. In contrast, Kupwade-Patil and Allouche [111], using the ASTM C1556 method, reported that AAFA concretes had lower chloride diffusion coefficients than their OPC-based counterparts. Ganesan [112] found that AAFA concrete performed comparably to cement-based concrete in terms of chloride resistance. Babaee and Castel [113] also reported comparable resistance for AAFA and OPC concrete when exposed to chloride medium. These variations are attributed to the complexity of chloride resistance in AAFA concrete and its sensitivity to various factors, including the activator type, testing methods, activator concentration, and fly ash fineness and reactivity.

Noushini [114] assessed the resistance of concrete with a low-calcium fly ash binder to chloride diffusion, cured at 60 ℃, 75 ℃, and 90 ℃ for 8, 12, 18, and 24 hours, using ASTM C1556 [115] and NT BUILD 492 [116] standards. Under the experimental conditions of this study, geopolymer concrete was reported to have limited resistance to chloride diffusion and a low chloride-binding capacity when fly ash was used as the sole binder. Curing at 75 ^{0}C for 18 to 24 enhances durability and chloride penetration resistance by decreasing the porosity and is also manifested by a reduction in the coefficient of sorptivity. A decrease in continuity of the pore system induced by appropriate heat curing is also reflected in increased electrical conductivity and mechanical strength. Conversely, heating for less than 75 ^{0}C and duration less than 18 hours increases the permeable porosity and sorptivity relative to curing at ambient laboratory conditions. Heat curing at 90 ^{0}C for 18-24 hours also reduced sorptivity and volume of interconnected pores compared to ambient curing.

4.1.2 Chloride Resistance of Alkali-activated GGBS

Runci and Serdar [117] observed that alkali-activated GGBS demonstrates exceptional resistance to chloride ingress, even with minimal curing duration. The chloride penetration resistance of AAS is strongly correlated with its capillary porosity and critical pore radius. While extended curing significantly influenced the overall porosity, it did not further enhance resistance to chloride transport. Notably, AAS achieved an exceptionally low chloride diffusion coefficient after just 7 days of curing, making it highly suitable for marine exposure and offering a distinct performance advantage over OPC-based concrete. However, it is important to consider that GGBS-based systems generally require a higher w/b ratio compared to fly ash-based systems. Increasing the water content can reduce chloride diffusion resistance [118], and increase the potential for drying shrinkage and cracking [119].

Adding a calcium source, such as calcium hydroxide ($Ca(OH)_2$), along with a high-alumina source, such as metakaolin, improves the capacity of mortar with an AAS binder to bind chlorides [120]. This is because the presence of additional supply Ca^{2+} from calcium hydroxide promotes and strengthens pozzolanic reaction of GGBS while Al^{3+} from metakaolin leads to formation of Alumino-ferrite monosubstituted (Afm) ($Ca_4Al_2O_6(SO_4)\cdot 14H_2O$) phases [120]. When carbonation is evident, the phase developed is Afm-CO_3. In the presence of Cl^{-1}, Afm transforms to Friedel's salt (Afm-Cl), a process that binds chloride. The partial replacement of 12% of the AAS binder with $Ca(OH)_2$ and metakaolin not only enhances the capacity to bind chlorides through the development of more C-A-S-H and development of Friedel's salt (Afm-Cl), but also increases compressive strength relative to control mortar samples. However, the source of additional calcium and alumina matters in terms of enhancing the chloride immobilization capacity of mortar with AAS binder. **Fig. 8**. shows that bound chloride in mortar with GGBS binder was highest when GGBS was partially replaced with 12% $Ca(OH)_2$ and metakaolin.

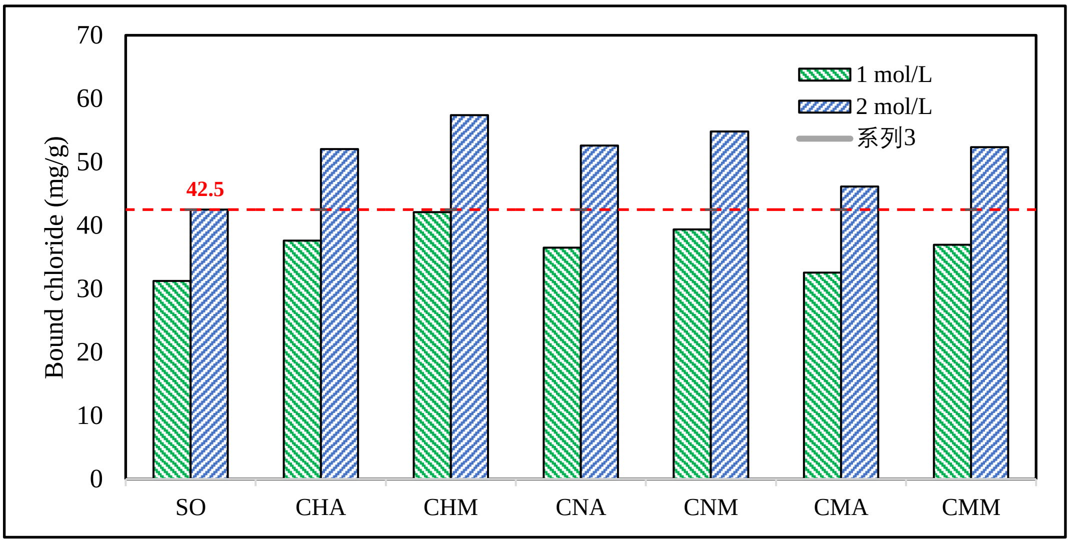

Fig. 8. Bound chloride in alkali-activated GGBS after immersion for 90 days in 2 mol/L chloride solution (CHM: calcium hydroxide+metakaolin; CHA: calcium hydroxide+ alpha-phase nano-alumna powder CNA: calcium nitrate + alpha-phase nano-alumina powder; CMM: cement+metakaolin) [120]

Zhang [121] conducted a comprehensive study on chloride resistance and binding behavior in unsaturated alkali-activated GGBS mortar samples. The findings indicated that reduced saturation slowed chloride diffusion but increased its penetration during wetting-drying cycles. GGBS mortars activated with NaOH exhibited a greater chloride-binding capacity than those activated using sodium silicate. This was attributed to the presence of more hydrotalcite-like phases and a higher Ca/Si ratio in C-(N-)A-S-H gels. GGBS is rich in CaO, SiO_2, Al_2O_3, and MgO. MgO and Al_2O_3 react in alkaline environment to form layered double hydroxide (LDH) that is similar to hydrotalcite ($[Mg_6Al_2(OH)_{16}]CO_3 \cdot 4H_2O$). Hydrotalcite-like phases in AAS mortar are effective in binding chloride ions. However, it is worth noting that incorporating 5% Mg-Al-CO_3 layered double hydroxide (LDH) increased air voids and decreased the mechanical strength of AASF-based mortar at all ages, compared to control samples based on OPC binder and without additives [122]. Therefore, the effect of Mg-based additives on AAMs depends on the type and dosage of the additive, among other factors.

Ye [123] found that AFm-type and hydrotalcite-like phases play a crucial role in binding chlorides in pastes with AAS binders, accounting for 40–70% of the overall chloride immobilization capacity. Additionally, the pH and characteristics of C-(N)-A-S-H gels significantly influence chloride immobilization mechanisms [124].

4.1.3 Chloride Resistance of Concrete with Fly Ash and GGBS Binders

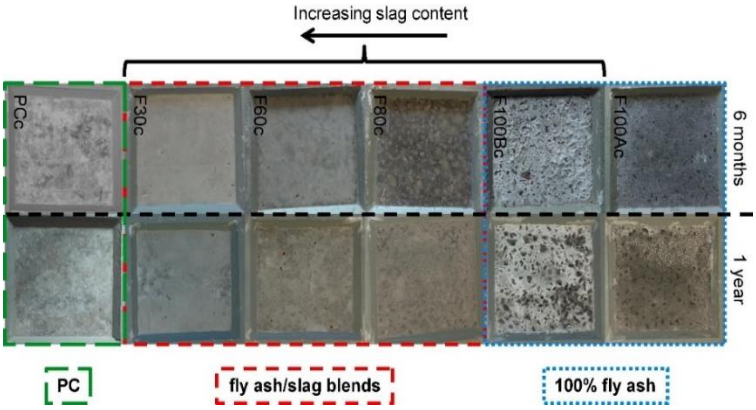

Fig. 9. Ponding surface of mixes after 6 months or 1 year of ponding in NaCl solution [48].

Similar to the enhancement noted in the resistance to carbonation obtained by blending GGBS and fly ash, literature also highlights that blending these materials enhances chloride resistance. Using NT

Build 492, Ismail [125] found that OPC-based materials had a greater chloride migration coefficient (CMC) than those containing blended AASF binders.

Concrete with an AAF binder exhibit high susceptibility to chloride migration due to the high VPV [48]. Conversely, increasing the GGBS content in fly/GGBS blends improved electrical resistivity and reduced VPV, resulting in a lower coefficient of chloride migration and decreased penetration depth. This improvement also enhanced the mechanical properties and reduced the corrosion of reinforcing steel bars. While OPC-based concrete showed superior ability to bind chlorides and enhanced protection against steel corrosion, GGBS-enriched alkali-activated blends offered comparable or superior resistance to chloride ingress. **Fig. 9** shows the ponding surfaces of various mixes after 6 months and 1 year of exposure to NaCl solution, illustrating the level of chloride penetration and highlighting the improved performance of GGBS-enriched blends in mitigating chloride ingress.

Fig. 10 illustrates a linear correlation, where the mix composed entirely of fly ash exhibited the highest capacity to bind chlorides, followed by the blend with a 50/50 GGBS-to-fly ash ratio [48]. Incorporating fly ash promotes the development of more N-A-S-H, potentially increasing the specific surface area of the gel phase, thereby improving chloride adsorption within the geopolymer matrix [125]. In contrast, mixtures containing 100% and 75% GGBS demonstrated reduced chloride binding capacity, attributed to the intrinsic properties of C-A-S-H gel, particularly its low Ca/Si ratio.

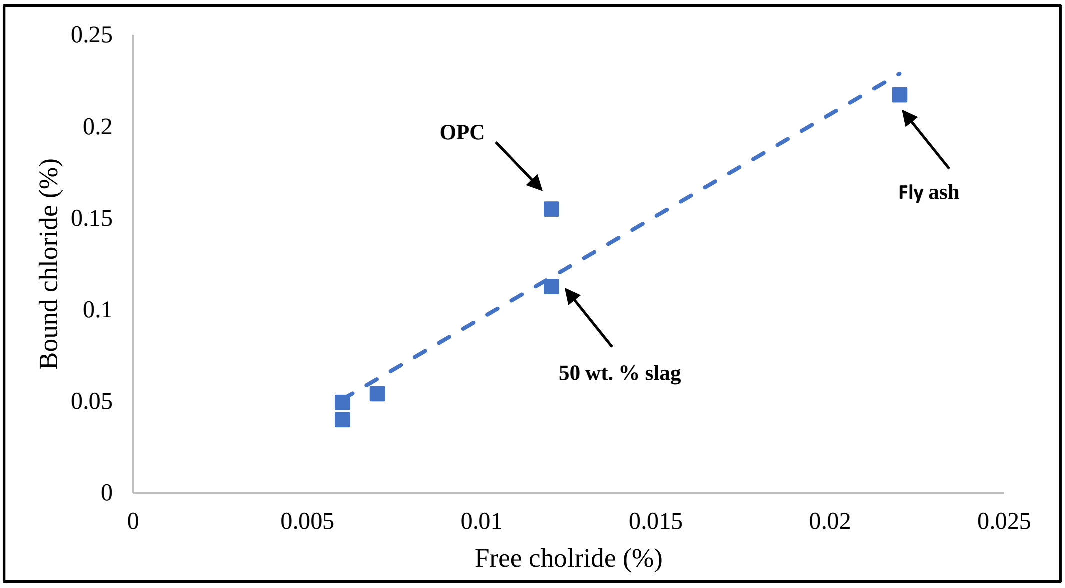

Fig. 10. Linear relationship between free and bound chlorides in OPC-based and alkali-activated binder [125].

Hu [104] investigated chloride transport in mortar with a GGBS binder, which was partially substituted by fly ash. GGBS was partially replaced by 20%, 40%, or 60% fly ash, and the impact on the CMC was evaluated using rapid chloride permeability (RCPT) and rapid chloride migration (RCMT) tests. Findings from both methods revealed a marginal rise in chloride permeability as fly ash content increased. Similarly, Fan [126] confirmed that lowering the FA content in alkali-activated GGBS concrete led to decreased chloride permeability. RCMT results indicated a notable reduction in chloride penetration in samples with a 50:50 fly ash-to-GGBS ratio relative to those composed solely of fly ash. Furthermore, the chloride permeability of mixtures made with 50%FA and 50% GGBS binders was found to be comparable to that of concrete with 100% GGBS binder.

4.2 Impact of Alkaline Activator Type and Concentration on Chloride Resistance of Concrete

The resistance of concrete and mortar with AABs to chloride penetration is highly impacted by the type of alkali activator, as well as its concentration. A higher concentration of alkali ions (Na^+, K^+, Ca^{2+}) from activators typically promotes precursor dissolution, accelerates geopolymerization, and leads to a more compact matrix, thereby enhancing resistance to chloride ingress [129, 128]. Alkali content is commonly represented by the molarity of metal hydroxides in the activating solution, such as 4M NaOH or 4M KOH, which supply a significant concentration of metal cations and hydroxide anions during activation. Alternatively, it can also be represented as the metal oxide content by mass relative to the precursor material, such as Na_2O to GGBS [124]. Higher alkali content facilitates the dissolution and hydration of precursors, thereby reducing porosity and enhancing chloride resistance.

Hu [104] found that increasing the alkali content from 2% to 8% accelerated the dissolution of AASF precursors, leading to a decrease in mortar porosity from approximately 16% to 10% and a reduction in the chloride migration coefficient from 3 to 1.5×10^{-12} m^2/s. However, excessive alkali content can adversely affect chloride resistance. Fang [127] showed that high alkali concentrations could lead to significant drying shrinkage and micro-cracking, undermining the material's resistance to chloride penetration.

The type of activator also plays a crucial role in chloride resistance. While the ability of concrete with AAS binder to bind chlorides is not solely determined by whether the activator is potassium- or sodium-based, differences exist in the amount of chlorides bound within the reacted phases. Sodium-activated binders typically show lower chloride binding in hydrotalcite-type and AFm-type phases than binders with potassium-based activators [123]. Sodium sulphate (Na_2SO_4) was particularly effective in increasing chloride binding capacity relative to other activators such as NaOH, Na_2CO_3, KOH, and K_2CO_3, leading to significantly higher bound chloride content in AAS pastes [105].

When using sodium-based activators, the gel phases exhibit enhanced chloride binding capacity, contributing to improved resistance to chloride ingress relative to those formed with potassium-based activators. This improvement is attributed to physical adsorption and chemisorption that contribute to immobilization of chloride ions [106]. Furthermore, increasing the Na_2O content in fly ash and GGBS AAM samples, while keeping SiO_2 content constant, reduced chloride diffusion by promoting faster precursor dissolution [48]. Conversely, increasing Na_2O content with a constant SiO_2/Na_2O ratio, which also increases SiO_2 content, resulting in higher chloride diffusion [107].

In addition to elevated alkali content, increased silica concentration further improves chloride resistance. An increased silica content in AAM systems, irrespective of the precursor type, helps decrease porosity and refine pore size distribution, thereby improving chloride-binding capacity [108]. Hu [104] confirmed that a higher silicate modulus enhances the compressive strength of AAM mortars by refining the pore network within the 10–104 nm range, thereby improving chloride resistance.

4.3 Effect of Curing Conditions

The curing duration critically governs the microstructural and mechanical evolution of conventional OPC systems, as well as blended binder systems [117]. However, while the overall porosity of AAS significantly decreased with longer curing durations, the chloride penetration resistance did not show a corresponding decrease. **Fig. 11** Illustrates that AAS exhibits lower chloride diffusivity within just 7 days of curing, demonstrating its strong potential for marine applications.

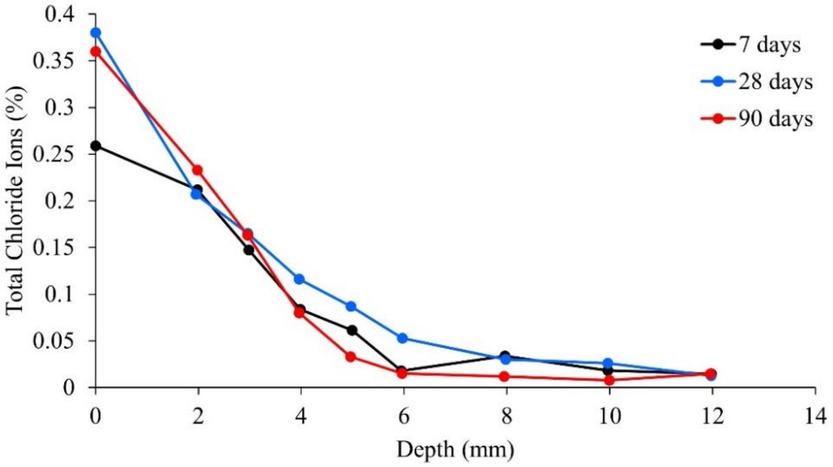

Fig. 11. Total chloride of AAS mortar cured for 7, 28 and 90 days, after 45 days of ponding [117].

Provis [128] established that extending the curing duration enhances tortuosity and decreases overall permeability, both of which play a critical role in controlling chloride diffusion. The curing method is essential for activating and refining the porosity characteristics in alkali-activated material systems. Curing at elevated temperatures typically result in reduced porosity and lower chloride ingress, especially in systems with AAF binder [114]. Furthermore, high-temperature curing improves GGBS reactivity, leading to reduced porosity and lower chloride permeability [129]. Incorporating GGBS to replace a predetermined percentage of OPC binder enhances the pozzolanic activity of the binder, facilitating the development of additional C-S-H and enhancing the binding capacity through physical adsorption, compared to OPC-only pastes [130]. Chen [130] reported that steam curing and standard curing have the same effect on the capacity of OPC pastes with partial GGBS or fly ash replacement to bind chlorides, while steam curing appears to enhance physical binding.

4.4 Chloride Penetration Testing Methods

4.4.1 Assessing Resistance of Concrete to Chlorides Using the Rapid Chloride Mitigation Test (RCMT)

The RCMT is standardized under the NordTest method NT Build 492 [116]. It is particularly effective for materials like AAMs, which possess complex pore solution chemistries due to the use of various alkali activators and precursors, as well as higher alkali concentrations [105]. The RCMT specifically measures chloride ion concentration within the mixture and is less affected by the presence of other ions, providing a more accurate assessment of chloride penetration in AAMs with elevated ionic strength or pore solution conductivity [105]. Unlike RCPT, RCMT results are less affected by variations in the pore structure or inconsistencies in solution chemistry.

4.4.2 Assessing Resistance of Concrete to Chlorides Using the Rapid Chloride Permeability Test (RCPT)

The RCPT, carried out in compliance with ASTM C1202/AASHTO T277 [131], is widely used to assess traditional OPC-based materials as well as AAMs [46]. This test evaluates the movement of electrical charge across a concrete specimen, which is affected by the concentration and chemical characteristics of the pore solution. In AAMs, the substantial ionic strength due to Na^+ and coexisting cations in the pore solution can influence RCPT outcomes. Although RCPT is effective for assessing variations in chloride permeability within geopolymer or AAM systems with similar pore solution chemistry, it does not reliably indicate overall concrete permeability across various concrete types due to differences in ion concentration and pore solution composition. The RCPT results can be skewed by the chemical nature of the pore solution, making it less consistent for AAMs with diverse chemistries [109]. **Table 2** presents selected studies on the resistance of concrete with AABs and/or OPC binders to chloride ion penetration, evaluated using various indicators such as total charge passed and chloride diffusion and migration coefficients.

Table 2. Summary of Studies on the Performance of Concrete with Alkali-Activated or OPC Binders Exposed to Chlorides (TCP: Total Charge Passed; CDC: Chloride Diffusion Coefficient; CMC: Chloride Migration Coefficient; CPD: Chloride Penetration Depth).

Parameter	Binder and Activator	Carbonation Conditions	Conclusion
TCP [132]	Binders: (1) OPC (2) 20% GGBS +80% OPC 80% Fly ash + 20% GGBS Activator: NaOH and Na_2SiO_3	Relative humidity maintained above 90% at 23 ℃	80% fly ash+20% GGBS concrete has low penetrability with 1100 coulombs of charge, and 20% GGBS replacement has very low penetrability with 300 coulombs, both performing better than OPC concrete which has 2400 coulombs, due to the presence of C-A-S-H and N-A-S-H gels, creating a denser microstructure.
CDC [133]	(1) OPC (2) 20% Fly ash + 80% OPC (3) 40% Fly ash + 60% OPC w/b ratio: 0.35, 0.45, 0.55, 0.65	Curing in water at 20 ℃	40% Fly ash + 60% OPC paste with a w/b ratio of 0.35 exhibited the lowest chloride diffusion coefficient (Dcl) of 3.101x10-8 cm^2/s at seven days, and this Dcl continued to decrease with increased curing age; higher water-to-binder ratios led to higher porosity and elevated Dcl, but as curing

			progressed and the material became denser, the effect of the w/b ratio on Dcl lessened.
CMC [134]	(1) OPC (2) 15% Fly ash + 85% OPC (3) 30% Fly ash + 70% OPC w/b ratio: 0.38, 0.47, 0.53	Curing in air under sealed conditions at a temperature (20 ℃)	15% Fly ash replacement in concrete reduces the chloride migration coefficient from 6.1x10-12 m^2/s to 4.2x10-12 m^2/s, while a 30% fly ash replacement lowers it further to 1.9x10-12 m^2/s. After 90 days of curing, the effects of fly ash stabilize. Higher w/b ratios increase the chloride migration due to increased porosity and interconnected capillaries.
CPD [36]	(1) OPC (2) 25% Fly ash + 75% OPC (3) 25% GGBS + 75% OPC w/b: 0.35, 0.45, 0.55, 0.65	Curing in air at 20 ℃	After 90 days, concrete with GGBS and fly ash had lower chloride penetration depths, with fly ash being more effective than GGBS. The chloride diffusion coefficient increased with a higher w/b ratio due to the formation of more pores but decreased with the use of fly ash and GGBS due to increased gel formation.
CDC [135]	(1) Fly ash & GGBS (20:80) (2) Fly ash &GGBS (40:60) (3) Fly ash & GGBS (60:40) (4) Fly ash & GGBS (80:20) Activator: NaOH + Na_2SiO_3 w/b: 0.47, 0.46, 0.44, 0.43	Curing in air. at 20 ℃	All concrete mixes had moderate to high chloride diffusion coefficients except for the one with an 80/20 GGBS/fly ash ratio, which exhibited reduced diffusivity. Average depth of chloride diffusion was 13 mm for the 20% fly ash+80% GGBS mix, and 40 mm for the 80% fly ash+ 20% GGBS mix.
CPD [125]	(1) OPC (2) 100% GGBS (3) 25% Fly ash +75% GGBS (4) 50% Fly ash + 50% GGBS Activator: NaOH + Na_2SiO_3	Curing in air. at 20 ℃	GGBS-based and 25% Fly ash + 75% GGBS had the lowest chloride penetration depths of 1 and 5 mm at 28 days. 50% Fly ash + 50% GGBS mortar had slightly higher depth, while OPC mortar had the highest, reaching 25 mm at 28 days. The chloride penetration depth significantly decreased with increased curing time from 28 to 90 days in AASF mortars, indicating that ongoing curing enhances the concrete's density and resistance to chloride ions
CPD [101]	(1) OPC (2) 100% GGBS (3) 90% Fly ash +10% GGBS (4)70% Fly ash + 30% GGBS (5) 50% Fly ash + 50% GGBS Activator: NaOH + Na_2SiO_3	Curing in air. at 20 ℃ and 50% RH.	50% GGBS and 50% fly ash binder had depths of 3.867 mm at 28 days and 7.736 mm at 91 days, whereas the 30% GGBS binder had depths of 8.361 mm and 14.428 mm at the same intervals. Higher GGBS content increased C-A-S-H gel, creating a more compact matrix and reducing chloride penetration, while larger fly ash content increased N-A-S-H gel, enhancing chloride binding but resulting in less dense matrices.
CPD [108]	(1) OPC (2) 100% GGBS (3) Fly ash: GGBS ratios of 70:30, 50: 50, and 30:70. Activator: NaOH + Na_2SiO_3 w/b ratios: 0.4, 0.45, 0.5	Curing in air at 20 ℃	Substituting 20–40% of fly ash with GGBS at a constant L/S ratio (0.7) has a limited effect on overall porosity but reduces pore sizes and increases tortuosity, thereby slowing chloride ion penetration and improving resistance to chloride ingress.
CDC [136]	(1) OPC (2) 100% GGBS (3) Fly ash: GGBS ratios of 70:30; 50:50; and 30:70	Curing in air at 20 ℃	In AAFS concrete, increasing GGBS content from 30% to 100% reduced the coefficient from 1.8x10-12 m^2/ to 0.4x10-12 m^2/s. When w/b was increased from 0.4

	Activator: NaOH + Na_2SiO_3 w/b ratios: 0.4, 0.45, 0.5		to 0.5, the 90-day chloride diffusion coefficient decreased from 3.19x10-12 m^2/s to 1.29x10-12 m^2/s
CDC [137]	(1) OPC (2) 100% GGBS (3) Fly ash: GGBS ratios of 70:30; 50:50; and 30:70 Activator: NaOH + Na_2SiO_3 with Na_2O percentages of 4%, 5%, and 6%. w/b ratio: 0.4, 0.45, 0.5	Curing in air at 20 ℃	Higher Na_2O content improved microstructure compactness, slightly reducing chloride diffusion, but its effect was less notable relative to the binder composition and w/b ratio.
CDC [138]	(1) OPC (2) Fly ash: GGBS = 75:25 (3) Fly ash: GGBS = 05:50 (4) Fly ash: GGBS = 25:75 Activator: NaOH + Na_2SiO_3 with Na_2O percentages of 3%, 5%, and 8%. Water to binder ratio: 0.35, 0.375, 0.4	Curing in air at 23 ℃ under sealed conditions.	Increasing Na_2O content in AASF increases the chloride diffusion coefficient. High SiO_2 contents, even with a constant SiO_2/Na_2O ratio, increases the diffusion coefficient by lowering the pH and reducing the degree of reaction.
CDC [118]	(1) OPC (2) 100% GGBS Activator: NaOH + Na_2SiO_3	Curing in air at 23 ℃ under dry conditions.	100% GGBS concretes exhibited smaller Chloride diffusion coefficients relative to OPC concrete. Chloride binding capacity measurements in 100% GGBS were affected by reduction in pH due to leaching, impacting a depth of 5 to 12 mm.
CDC [111]	(1) Fly ash (ASTM Class F) (2) Fly ash (ASTM Class C) Activator: NaOH + Na_2SiO_3	Curing in water then exposure to 7.5% NaCl concentration	Class C Fly ash contains more calcium than Class F Fly ash, promoting development of calcium chlorides ($CaCl_2$) and Friedel's salt. This can lead to chloride dissolution and rebar corrosion.
CDC [111]	(1) Fly ash (ASTM Class F) (2) Fly ash (ASTM Class C) Activator: NaOH + Na_2SiO_3	Curing in water then exposure to 7.5% NaCl concentration	After 150 days, Class F Fly ash recorded 1,652 coulombs (low penetrability) while Class C Fly ash and OPC specimens recorded 10,204 and 10,931 coulombs, respectively (high penetrability).
CDC [139]	(1) OPC (2) 100% GGBS Activator: NaOH + Na_2SiO_3 with 8% Na_2O.	Curing in water then exposure to 5% NaCl concentration	Compared to OPC concrete, 100% GGBS concrete exhibited greater resistance to chloride ingress. 8% of Na_2O helped maintain long-term alkalinity, effectively preventing corrosion.

5 Conclusion

The durability, long-term integrity, and service life of concrete structures that use ordinary Portland cement (OPC) or binders activated in an alkaline medium are influenced by the corrosion of steel reinforcement caused by chloride ingress or carbonation. Therefore, it is essential to understand the carbonation and chloride ingress mechanisms in concrete made with OPC, OPC that is partially replaced with GGBS and fly ash binders, or GGBS and fly ash binders activated in an alkaline medium. Slag and fly ash are utilized as alkali-activated binders or OPC substitutes, contributing to enhanced concrete performance while simultaneously mitigating environmental impact through reduced OPC consumption and the beneficial reuse of these industrial byproducts.

- Alkali-activated binders with higher calcium content exhibit better carbonation resistance and CO_2 absorption. Combining GGBS with fly ash enhances the carbonation resistance compared to using each material separately.

- Mortar with binder activated using sodium silicate exhibit better carbonation than those activated with NaOH.
- Sealed curing enhances carbonation resistance, particularly for mortar with alkali-activated GGBS binder.
- Accelerated carbonation curing improves mechanical properties and reduces carbon footprints.
- Combining alkali-activated GGBS with fly ash improves chloride resistance of concrete and mortar, compared to 100% fly ash mixtures. GGBS enhances mechanical properties and reduces chloride ingress in concrete, thereby mitigating the corrosion of embedded steel.
- Concrete developed with binders activated by sodium-based compounds exhibits superior chloride binding capacity compared to those utilizing potassium-based activators.
- Longer curing durations and higher curing temperature improve the chloride penetration resistance by reducing porosity and enhancing pore structure.
- In concrete/mortar with alkali-activated binders, the molarity or dosage of the alkaline activator affects the porosity and chloride resistance of the binder, with higher concentrations leading to better performance.

Funding Statement

O.A.M acknowledges the financial support provided by the Office of Research and Sponsored Programs (ORSP) at Abu Dhabi University under grant #19300899.

CRediT authorship contribution statement

Osama A. Mohamed: Conceptualization, Funding Acquisition, Writing – original draft. **Haya Zuaiter**: Investigation, Supervision, Formal analysis, Writing – review & editing. **Muhammad Jawa**: Investigation, Formal Analysis, Writing – review & editing.

Conflicts of Interest

The authors declare that they have no conflicts of interest to report regarding the present study.

References

[1] Habert G, Ouellet-Plamondon C. Recent update on the environmental impact of geopolymers. RILEM Technical Letters 1 (2016) 17–23. https://doi.org/10.21809/rilemtechlett.2016.6.

[2] Siddique R, Khan MI. Supplementary Cementing Materials, Springer Berlin Heidelberg. Berlin, Heidelberg, 2011. https://doi.org/10.1007/978-3-642-17866-5.

[3] van Deventer JSJ, Provis JL, Duxson P, Brice DG. Chemical Research and Climate Change as Drivers in the Commercial Adoption of Alkali Activated Materials. Waste Biomass Valorization 1 (2010) 145–155. https://doi.org/10.1007/s12649-010-9015-9.

[4] Van Deventer JSJ, Provis JL, Duxson P. Technical and commercial progress in the adoption of geopolymer cement. Miner Eng 29 (2012) 89–104. https://doi.org/10.1016/j.mineng.2011.09.009.

[5] Arbi K, Nedeljković M, Zuo Y, Ye G. A Review on the Durability of Alkali-Activated Fly Ash/Slag Systems: Advances, Issues, and Perspectives. Ind Eng Chem Res 55 (2016) 5439–5453. https://doi.org/10.1021/acs.iecr.6b00559.

[6] Parrott LJ. Damage caused by carbonation of reinforced concrete, Mater Struct 23 (1990) 230–234. https://doi.org/10.1007/BF02473023.

[7] Bertolini L, Elsener B, Pedeferri P, Redaelli E, Polder RB. Corrosion of Steel in Concrete. Wiley, 2013. https://doi.org/10.1002/9783527651696.

[8] Bernal SA, Provis JL, Walkley B, San Nicolas R, Gehman JD, Brice DG, Kilcullen AR, Duxson P, van Deventer JSJ. Gel nanostructure in alkali-activated binders based on slag and fly ash, and effects of accelerated carbonation. Cem Concr Res 53 (2013) 127–144. https://doi.org/10.1016/j.cemconres. 2013.06.007.

[9] Duxson P, Mallicoat SW, Lukey GC, Kriven WM, van Deventer JSJ. The effect of alkali and Si/Al ratio on the development of mechanical properties of metakaolin-based geopolymers. Colloids Surf A Physicochem Eng Asp 292 (2007) 8–20. https://doi.org/10.1016/j.colsurfa.2006.05.044.

[10] Duxson P, Fernández-Jiménez A, Provis JL, Lukey GC, Palomo A, Van Deventer JSJ. Geopolymer

technology: The current state of the art. J Mater Sci 42 (2007) 2917–2933. https://doi.org/10. 1007/s10853-006-0637-z.

[11] Wu Y, Lu B, Bai T, Wang H, Du F, Zhang Y, Cai L, Jiang C, Wang W. Geopolymer, green alkali activated cementitious material: Synthesis, applications and challenges. Constr Build Mater 224 (2019) 930–949. https://doi.org/10.1016/j.conbuildmat.2019.07.112.

[12] Lahoti M, Tan KH, Yang EH. A critical review of geopolymer properties for structural fire-resistance applications. Constr Build Mater 221 (2019) 514–526. https://doi.org/10.1016/j.conbuildmat. 2019.06.076.

[13] Marvila MT, de Azevedo ARG, Vieira CMF. Reaction mechanisms of alkali-activated materials. Revista IBRACON de Estruturas e Materiais 14 (2021). https://doi.org/10.1590/s1983-41952021000300009.

[14] Rożek P, Król M, Mozgawa W. Geopolymer-zeolite composites: A review. J Clean Prod 230 (2019) 557–579. https://doi.org/10.1016/j.jclepro.2019.05.152.

[15] Lamaa G, Duarte APC, Silva RV, de Brito J. Carbonation of Alkali-Activated Materials: A Review. Materials 16 (2023) 3086. https://doi.org/10.3390/ma16083086.

[16] Zuaiter M, El-Hassan H, El-Maaddawy T, El-Ariss B. Properties of Slag-Fly Ash Blended Geopolymer Concrete Reinforced with Hybrid Glass Fibers. Buildings 12 (2022) 1114. https://doi.org/10.3390/b uildings 12081114.

[17] Palomo A, Grutzeck MW, Blanco MT. Alkali-activated fly ashes. Cem Concr Res 29 (1999) 1323–1329. https://doi.org/10.1016/S0008-8846(98)00243-9.

[18] Dhir R, and Byars EA. Pulverized Fuel-Ash Concrete: Intrinsic Permeability. ACI Materials Journal, American Concrete Institute 90 (1993).

[19] Hench LL, West JK. The sol-gel process. Chem Rev 90 (1990) 33–72. https://doi.org/10.1021/cr00099a003.

[20] Sindhunata, van Deventer JSJ, Lukey GC, Xu H. Effect of Curing Temperature and Silicate Concentration on Fly-Ash-Based Geopolymerization. Ind Eng Chem Res 45 (2006) 3559–3568. https://doi.org/10.1021/ie051251p.

[21] van Jaarsveld JGS, van Deventer JSJ, Lukey GC. The characterization of source materials in fly ash-based geopolymers. Mater Lett 57 (2003) 1272–1280. https://doi.org/10.1016/S0167-577X(02)00971-0.

[22] Mohamed OA. Effect of mix constituents and curing conditions on compressive strength of sustainable self-consolidating concrete. Sustainability (Switzerland) 11 (2019). https://doi.org/10.3390/su1102094.

[23] Mohamed O. Durability and compressive strength of high cement replacement ratio self-consolidating concrete. Buildings 8 (2018). https://doi.org/10.3390/buildings8110153.

[24] Angulo-Ramírez DE, Mejía de Gutiérrez R, Puertas F. Alkali-activated Portland blast-furnace slag cement: Mechanical properties and hydration. Constr Build Mater 140 (2017) 119–128. https://doi.org/10.1016/j.conbuildmat.2017.02.092.

[25] Pacheco-Torgal F, Labrincha JA, Leonelli C, Palomo A, Chindaprasirt P. Handbook of Alkali-Activated Cements, Mortars and Concretes, Elsevier, 2015. https://doi.org/10.1016/C2013-0-16511-7.

[26] Chang JJ. A study on the setting characteristics of sodium silicate-activated slag pastes. Cem Concr Res 33 (2003) 1005–1011. https://doi.org/10.1016/S0008-8846(02)01096-7.

[27] Nath P, Sarker PK. Effect of GGBFS on setting, workability and early strength properties of fly ash geopolymer concrete cured in ambient condition. Constr Build Mater 66 (2014) 163–171. https://doi.org/10. 1016/j.conbuildmat.2014.05.080.

[28] Ben Haha M, Le Saout G, Winnefeld F, Lothenbach B. Influence of activator type on hydration kinetics, hydrate assemblage and microstructural development of alkali activated blast-furnace slags. Cem Concr Res 41 (2011) 301–310. https://doi.org/10.1016/j.cemconres.2010.11.016.

[29] Puertas F, Varga C, Palacios M, Pellerin B, Eychenne-Baron C, Babayan D, Boustingorry P, Elkhadiri I. Alkali-activation of slag cements: Activation process, microstructure and mechanical properties. in: Proceedings of 13th International Congress on the Chemistry of Cement, 2011: pp. 3–8.

[30] Bilim C, Atiş CD. Alkali activation of mortars containing different replacement levels of ground granulated blast furnace slag. Constr Build Mater 28 (2012) 708–712. https://doi.org/10.1016/j.conbuild mat.2011. 10.018.

[31] Mohamed OA, Najm OF. Splitting tensile strength of self-consolidating concrete containing slag, in: AES-ATEMA International Conference Series - Advances and Trends in Engineering Materials and Their Applications, 2016: pp. 109–114.

[32] Fernandez-Jimenez A, Flores E, Maltseva O, Garcia-Lodeiro I, Palomo A. Hybrid alkaline cements: Part III Durability and industrial applications. Romanian Journal of Materials 43 (2013) 68–73.

[33] Bernal SA, Mejía de Gutiérrez R, Pedraza AL, Provis JL, Rodriguez ED, Delvasto S. Effect of binder content on the performance of alkali-activated slag concretes. Cem Concr Res 41 (2011) 1–8. https://doi.org/10.1016/j.cemconres.2010.08.017.

[34] Bellmann F, Stark J. Activation of blast furnace slag by a new method. Cem Concr Res 39 (2009) 644–650. https://doi.org/10.1016/j.cemconres.2009.05.012.

[35] Law DW, Adam AA, Molyneaux TK, Patnaikuni I. Durability assessment of alkali activated slag (AAS)

concrete. Mater Struct 45 (2012) 1425–1437. https://doi.org/10.1617/s11527-012-9842-1.
[36] Yang T, Yao X, Zhang Z. Quantification of chloride diffusion in fly ash–slag-based geopolymers by X-ray fluorescence (XRF). Constr Build Mater 69 (2014) 109–115. https://doi.org/10.1016/j.conb uildmat.2014.07 .031.
[37] Puertas F, Palacios M, Vázquez T. Carbonation process of alkali-activated slag mortars. J Mater Sci 41 (2006) 3071–3082. https://doi.org/10.1007/s10853-005-1821-2.
[38] Shi C, Jiménez AF, Palomo A. New cements for the 21st century: The pursuit of an alternative to Portland cement, Cem Concr Res 41 (2011) 750–763. https://doi.org/10.1016/j.cemconre s.2011. 03.016.
[39] Bakharev T. Geopolymeric materials prepared using Class F fly ash and elevated temperature curing. Cem Concr Res 35 (2005) 1224–1232. https://doi.org/10.1016/j.cemconres.2004.06.031.
[40] Collins FG, Sanjayan JG. Workability and mechanical properties of alkali activated slag concrete. Cem Concr Res 29 (1999) 455–458. https://doi.org/10.1016/S0008-8846(98)00236-1.
[41] Shi C, Qu B, Provis JL. Recent progress in low-carbon binders. Cem Concr Res 122 (2019) 227–250. https://doi.org/10.1016/j.cemconres.2019.05.009.
[42] El-Hassan H, Elkholy S. Performance Evaluation and Microstructure Characterization of Steel Fiber–Reinforced Alkali-Activated Slag Concrete Incorporating Fly Ash. Journal of Materials in Civil Engineering 31 (2019). https://doi.org/10.1061/(ASCE)MT.1943-5533.0002872.
[43] Rafeet A, Vinai R, Soutsos M, Sha W. Effects of slag substitution on physical and mechanical properties of fly ash-based alkali activated binders (AABs). Cem Concr Res 122 (2019) 118–135. https://doi.org/10.1016/ j.cemconres.2019.05.003.
[44] Palomo A, Tseva OM, Garcia-Lodeiro I. A. Fernandez-Jimenez, Hybrid alcaline cements. Part II: the clinker factor. Revista Română de Materiale / Romanian Journal of Materials 43 (2013) 74–80.
[45] Garcia-Lodeiro I, Fernandez-Jimenez A, Palomo A. Hydration kinetics in hybrid binders: Early reaction stages. Cem Concr Compos 39 (2013) 82–92. https://doi.org/10.1016/j.cemconco mp.2013.03.025.
[46] Ma Y, Hu J, Ye G. The pore structure and permeability of alkali activated fly ash. Fuel 104 (2013) 771–780. https://doi.org/10.1016/j.fuel.2012.05.034.
[47] Wardhono A, Gunasekara C, Law DW, Setunge S. Comparison of long term performance between alkali activated slag and fly ash geopolymer concretes. Constr Build Mater 143 (2017) 272–279. https://doi.org /10. 1016/j.conbuildmat.2017.03.153.
[48] Aiken TA, Kwasny J, Sha W, Tong KT. Mechanical and durability properties of alkali-activated fly ash concrete with increasing slag content. Constr Build Mater 301 (2021) 124330. https://doi.or g/10.1016/j.con buildmat.2021.124330.
[49] Nedeljković M, Li Z, Ye G. Setting, Strength, and Autogenous Shrinkage of Alkali-Activated Fly Ash and Slag Pastes: Effect of Slag Content. Materials 11 (2018) 2121. https://doi.org/10.3390/ ma11112121.
[50] Mohamed OM, Najm O, Ahmed E. Alkali-activated slag & fly ash as sustainable alternatives to OPC: Sorptivity and strength development characteristics of mortar. Cleaner Materials 8 (2023) 100188. https: //do i.org/10.1016/j.clema.2023.100188.
[51] Liao G, Wang D, Wang W, He Y. Microstructure, strength development mechanism, and CO2 emission analyses of alkali-activated fly ash-slag mortars. J Clean Prod 442 (2024) 141116. https://doi.org/10.1016/j.jclepro.2024.141116.
[52] Mohamed OA, Al Khattab R, Al Hawat W. Effect of relative GGBS/fly contents and alkaline solution concentration on compressive strength development of geopolymer mortars subjected to sulfuric acid. Sci Rep 12 (2022). https://doi.org/10.1038/s41598-022-09682-z.
[53] Mohamed OA, Al-Khattab R, Al-Hawat W. Resistance to acid degradation, sorptivity, and setting time of geopolymer mortars. Frontiers of Structural and Civil Engineering 16 (2022) 781–791. https://doi.org/10.10 07/s11709-022-0862-9.
[54] Mohamed OA, Najm O, Zuaiter HA. Setting time, sulfuric acid resistance, and strength development of alkali-activated mortar with slag & fly ash binders. Results in Engineering 21 (2024) 101711. https://doi.org/10.1016/j.rineng.2023.101711.
[55] Samantasinghar S, Singh S. Effects of curing environment on strength and microstructure of alkali-activated fly ash-slag binder. Constr Build Mater 235 (2020). https://doi.org/10.1016/j.conbuildm at.2019.117481.
[56] Ma H, Fu H, Cao C, Xu Z, Niu X. Effect of 60 °C sustained temperature conditions on the mechanical properties and microstructure of alkali-activated fly ash-slag pastes and mortars. Journal of Building Engineering 95 (2024) 110346. https://doi.org/10.1016/j.jobe.2024.110346.
[57] Tu W, Fang G, Dong B, Zhang M. Micromechanical analysis of alkali-activated fly ash-slag paste subjected to elevated temperatures. Cem Concr Compos 153 (2024) 105735. https://doi.org/10.1016/j. cemconcomp. 2024.105735.
[58] Papadakis V, Vayenas C, Fardis M. Physical and chemical characteristics affecting the durability of concrete. ACI Mater J 88 (1991) 186–196.
[59] Castel A, François R, Arliguie G. Effect of loading on carbonation penetration in reinforced concrete

elements. Cem Concr Res 29 (1999) 561–565. https://doi.org/10.1016/S0008-8846(99)00017-4.

[60] Hwalla J, Al-Mazrouei M, Al-Karbi K, Al-Hebsi A, Al-Ameri M, Al-Hadrami F, El-Hassan H. Performance of Alkali-Activated Slag Concrete Masonry Blocks Subjected to Accelerated Carbonation Curing. Sustainability 15 (2023) 14291. https://doi.org/10.3390/su151914291.

[61] Rashad AM. A synopsis of carbonation of alkali-activated materials. Green Mater 7 (2019) 118–136. https: //doi.org/10.1680/jgrma.18.00052.

[62] Bernal SA, San Nicolas R, Myers RJ, Mejía de Gutiérrez R, Puertas F, van Deventer JSJ, Provis JL. MgO content of slag controls phase evolution and structural changes induced by accelerated carbonation in alkali-activated binders. Cem Concr Res 57 (2014) 33–43. https://doi.org/10.1016/j.cemconres.2013.12.003.

[63] Cultrone G, Sebastián E, Huertas MO. Forced and natural carbonation of lime-based mortars with and without additives: Mineralogical and textural changes. Cem Concr Res 35 (2005) 2278–2289. https://doi.org/10.1016/j.cemconres.2004.12.012.

[64] Morandeau A, Thiéry M, Dangla P. Investigation of the carbonation mechanism of CH and C-S-H in terms of kinetics, microstructure changes and moisture properties. Cem Concr Res 56 (2014) 153–170. https://doi.org/10.1016/j.cemconres.2013.11.015.

[65] Badar MS, Kupwade-Patil K, Bernal SA, Provis JL, Allouche EN. Corrosion of steel bars induced by accelerated carbonation in low and high calcium fly ash geopolymer concretes. Constr Build Mater 61 (2014) 79–89. https://doi.org/10.1016/j.conbuildmat.2014.03.015.

[66] Liu S, Hao Y, Ma G. Approaches to enhance the carbonation resistance of fly ash and slag based alkali-activated mortar- experimental evaluations. J Clean Prod 280 (2021) 124321. https://doi.org/10.1016/j.jclepro.2020.124321.

[67] Charitha V, Athira G, Bahurudeen A, Shekhar S. Carbonation of alkali activated binders and comparison with the performance of ordinary Portland cement and blended cement binders. Journal of Building Engineering 53 (2022) 104513. https://doi.org/10.1016/j.jobe.2022.104513.

[68] You D. Preparation and properties of alkali-activated cement containing phosphorus slag and fly ash. Ceramics - Silikaty (2016) 63–67. https://doi.org/10.13168/cs.2016.0009.

[69] Khan MSH, Castel A, Noushini A. Carbonation of a low-calcium fly ash geopolymer concrete. Magazine of Concrete Research 69 (2017) 24–34. https://doi.org/10.1680/jmacr.15.00486.

[70] Nedeljković M, Šavija B, Zuo Y, Luković M, Ye G. Effect of natural carbonation on the pore structure and elastic modulus of the alkali-activated fly ash and slag pastes. Constr Build Mater 161 (2018) 687–704. https://doi.org/10.1016/j.conbuildmat.2017.12.005.

[71] Huseien GF, Shah HW. Durability and life cycle evaluation of self-compacting concrete containing fly ash as GBFS replacement with alkali activation. Constr Build Mater 235 (2020) 117458. https: /doi.org/10.10/16/j.conbuildmat.2019.117458.

[72] Huy Vu Q, Pham G, Chonier A, Brouard E, Rathnarajan S, Pillai R, Gettu R, Santhanam M, Aguayo F, Folliard KJ, Thomas MD, Moffat T, Shi C, Sarnot A. Impact of different climates on the resistance of concrete to natural carbonation. Constr Build Mater 216 (2019) 450–467. https://doi.org/10.1016/j.conbuildmat.2019.04.263.

[73] Li N, Farzadnia N, Shi C. Microstructural changes in alkali-activated slag mortars induced by accelerated carbonation. Cem Concr Res 100 (2017) 214–226. https://doi.org/10.1016/j.c emconres.2017.07.008.

[74] Bernal SA, de Gutierrez RM, Provis JL, Rose V. Effect of silicate modulus and metakaolin incorporation on the carbonation of alkali silicate-activated slags. Cem Concr Res 40 (2010) 898–907. https://doi.org/10.1016/j.cemconres.2010.02.003.

[75] Nedeljković M, Ghiassi B, van der Laan S, Li Z, Ye G. Effect of curing conditions on the pore solution and carbonation resistance of alkali-activated fly ash and slag pastes. Cem Concr Res 116 (2019) 146–158. https://doi.org/10.1016/j.cemconres.2018.11.011.

[76] Mo L, Panesar DK. Effects of accelerated carbonation on the microstructure of Portland cement pastes containing reactive MgO. Cem Concr Res 42 (2012) 769–777. https://doi.org/10.1016/j.cemconres. 2012. 02.017.

[77] Provis JL, van Deventer JSJ. Alkali Activated Materials: State-of-the-Art Report, RILEM TC 224-AAM. Springer Netherlands, Dordrecht, 2014. https://doi.org/10.1007/978-94-007-7672-2.

[78] Wang Z, Park S, Khalid HR, Kim S, Lee HK. Carbonation behavior of aged alkali-activated fly ash/slag binder modified by MgO with different reactivities. Mater Struct 57 (2024) 119. https:// doi.org/10.1617/s11527-024-02397-9.

[79] Wang SD, Scrivener KL. Hydration products of alkali activated slag cement. Cem Concr Res 25 (1995) 561–571. https://doi.org/10.1016/0008-8846(95)00045-E.

[80] Fernández-Jiménez A, Palomo JG, Puertas F. Alkali-activated slag mortars, Cem Concr Res 29 (1999) 1313–1321. https://doi.org/10.1016/S0008-8846(99)00154-4.

[81] Morales-Florez V, Findling N, Brunet F. Changes on the nanostructure of cementitius calcium silicate hydrates (C–S–H) induced by aqueous carbonation. J Mater Sci 47 (2012) 764–771. https://doi.org/10. 100

7/s10853-011-5852-6.

[82] Sevelsted TF, Skibsted J. Carbonation of C–S–H and C–A–S–H samples studied by 13 C, 27 Al and 29 Si MAS NMR spectroscopy. Cem Concr Res 71 (2015) 56–65. https://doi.org/10.1016/j.cemconre s.2015. 01. 019.

[83] Avila Y, Silva RV, de Brito J. Alkali-Activated Materials with Pre-Treated Municipal Solid Waste Incinerator Bottom Ash. Applied Sciences 12 (2022) 3535. https://doi.org/10.3390/app12073535.

[84] Kassim D, Lamaa G, Silva RV, de Brito J. Performance Enhancement of Alkali-Activated Electric Arc Furnace Slag Mortars through an Accelerated CO2 Curing Process. Applied Sciences 12 (2022) 1662. https ://doi.org/10.3390/app12031662.

[85] Zhang J, Shi C, Zhang Z. Effect of Na2O concentration and water/binder ratio on carbonation of alkali-activated slag/fly ash cements. Constr Build Mater 269 (2021). https://doi.org/10.1016/j.con buildmat.2020. 121258.

[86] Morone M, Cizer Ö, Costa G, Baciocchi R. Effects of Alkali Activation and CO2 Curing on the Hydraulic Reactivity and Carbon Storage Capacity of BOF Slag in View of Its Use in Concrete. Waste Biomass Valorization 11 (2020) 3007–3020. https://doi.org/10.1007/s12649-019-00579-z.

[87] Behfarnia K, Rostami M. An assessment on parameters affecting the carbonation of alkali-activated slag concrete. J Clean Prod 157 (2017) 1–9. https://doi.org/10.1016/j.jclepro.2017.04.097.

[88] Mohamed OA. Effect of immersing geopolymer slag-fly ash mortar in sulfuric acid on strength development and stability of mass. Constr Build Mater 341 (2022) 127786. https://doi.org/10.1016/j.conbuildma t.2022. 127786.

[89] Liu Z, Meng W. Fundamental understanding of carbonation curing and durability of carbonation-cured cement-based composites: A review. Journal of CO2 Utilization 44 (2021) 101428. https:// doi.org/10.1016/j. jcou.2020.101428.

[90] El-Hassan H, Shao Y, Ghouleh Z. Effect of Initial Curing on Carbonation of Lightweight Concrete Masonry Units. ACI Mater J 110 (2013). https://doi.org/10.14359/51685791.

[91] Hu Y, Tang Z, Li W, Li Y, Tam VWY. Physical-mechanical properties of fly ash/GGBFS geopolymer composites with recycled aggregates. Constr Build Mater 226 (2019) 139–151. https://doi.org/10.1016/j.con buildmat.2019.07.211.

[92] Huang Q, Shi X, Wang Q, Tang L. The Influence of Carbonization on the Performances of Fly Ash Geopolymeric Concrete. Applied Mechanics and Materials 744–746 (2015) 1519–1526. https://do i.org/10. 4028/www.scientific.net/AMM.744-746.1519.

[93] Pasupathy K, Berndt M, Castel A, Sanjayan J, Pathmanathan R. Carbonation of a blended slag-fly ash geopolymer concrete in field conditions after 8 years. Constr Build Mater 125 (2016) 661–669. https://doi.o rg/10.1016/j.conbuildmat.2016.08.078.

[94] Deja J. Carbonation aspects of alkali activated slag mortars and concretes. Silicates Industriels 3 (2002) 37–42.

[95] Bakharev T, Sanjayan JG, Cheng YB. Resistance of alkali-activated slag concrete to carbonation, Cem Concr Res 31 (2001) 1277–1283. https://doi.org/10.1016/S0008-8846(01)00574-9.

[96] Yang KH, Seo EA, Tae SH. Carbonation and CO2 uptake of concrete. Environ Impact Assess Rev 46 (2014) 43–52. https://doi.org/10.1016/j.eiar.2014.01.004.

[97] Bernal SA, Provis JL. Durability of Alkali-Activated Materials: Progress and Perspectives. Journal of the American Ceramic Society 97 (2014) 997–1008. https://doi.org/10.1111/jace.12831.

[98] Chen JJ, Thomas JJ, Jennings HM. Decalcification shrinkage of cement paste. Cem Concr Res 36 (2006) 801–809. https://doi.org/10.1016/j.cemconres.2005.11.003.

[99] Xu H, Provis JL, van Deventer JSJ, Krivenko PV. Characterization of Aged Slag Concretes. ACI Mater J 105 (2008). https://doi.org/10.14359/19753.

[100] Nedeljković M, Zuo Y, Arbi K, Ye G. Carbonation Resistance of Alkali-Activated Slag Under Natural and Accelerated Conditions. Journal of Sustainable Metallurgy 4 (2018) 33–49. https://doi.org/10.1007/s40831-018-0166-4.

[101] Lee NK, Lee HK. Influence of the slag content on the chloride and sulfuric acid resistances of alkali-activated fly ash/slag paste. Cem Concr Compos 72 (2016) 168–179. https://doi.org/10.1016/j.cemc oncomp .2016.06.004.

[102] Pu XC, Gan CC, Wang SD, Yang CH. Summary reports of research on alkali-activated slag cement and concrete. Chongqing, 1988.

[103] Qiao C, Ni W, Wang Q, Weiss J. Chloride Diffusion and Wicking in Concrete Exposed to NaCl and MgCl2 Solutions. Journal of Materials in Civil Engineering 30 (2018). https://doi.org/10.1061/(A SCE)MT. 1943-5533.0002192.

[104] Hu X, Shi C, Shi Z, Zhang L. Compressive strength, pore structure and chloride transport properties of alkali-activated slag/fly ash mortars. Cem Concr Compos 104 (2019). https://doi.org/10.1016/j.cemconcom p.2019.103392.

[105] Thunuguntla CS, Gunneswara Rao TD. Effect of mix design parameters on mechanical and durability properties of alkali activated slag concrete. Constr Build Mater 193 (2018) 173–188. https://doi.org/10.1016/j.conbuildmat.2018.10.189.

[106] Zhang J, Shi C, Zhang Z, Ou Z. Durability of alkali-activated materials in aggressive environments: A review on recent studies. Constr Build Mater 152 (2017) 598–613. https://doi.org/10.1016/j.conbuild mat.2017.07.027.

[107] Angst U, Elsener E, Larsen CK, Vennesland Ø. Critical chloride content in reinforced concrete — A review. Cem Concr Res 39 (2009) 1122–1138. https://doi.org/10.1016/j.cemcon res.2009.08.006.

[108] Zhu H, Zhang Z, Zhu Y, Tian L. Durability of alkali-activated fly ash concrete: Chloride penetration in pastes and mortars. Constr Build Mater 65 (2014) 51–59. https://doi.org/10. 1016/j.conbuildmat.2014.04.110.

[109] Olivia M, Nikraz H. Durability of fly ash geopolymer concrete in a seawater environment, in: Proceedings of the CONCRETE 2011 Conference, The Concrete Institute of Australia, 2011.

[110] Provis JL, Bernal SA. Milestones in the analysis of alkali-activated binders, J Sustain Cem Based Mater 4 (2015) 74–84. https://doi.org/10.1080/21650373.2014.958599.

[111] Kupwade-Patil K, Allouche EN. Examination of Chloride-Induced Corrosion in Reinforced Geopolymer Concretes. Journal of Materials in Civil Engineering 25 (2013) 1465–1476. https://doi.org/10.1061/(ASC E)MT.1943-5533.0000672.

[112] Ganesan N, Abraham R, Deepa Raj S. Durability characteristics of steel fibre reinforced geopolymer concrete. Constr Build Mater 93 (2015) 471–476. https://doi.org/10.1016/j.conbuildmat.2015.06.014.

[113] Babaee M, Castel A. Chloride-induced corrosion of reinforcement in low-calcium fly ash-based geopolymer concrete. Cem Concr Res 88 (2016) 96–107. https://doi.org/10.1016/j.cemconres.2016.05.012.

[114] Noushini A, Castel A. The effect of heat-curing on transport properties of low-calcium fly ash-based geopolymer concrete. Constr Build Mater 112 (2016) 464–477. https://doi.org/10.1016/j.conbuildmat.2016.02.210.

[115] ASTM C1698. Test Method for Autogenous Strain of Cement Paste and Mortar, (2019). https://doi.org/10.1520/C1698-19.

[116] Nordtest: NT BUILD 492. NT BUILD 492: Concrete, chloride migration coefficient from non-steady-state migration experiments, Nordic Innovation, 1999.

[117] Runci A, Serdar M. Effect of curing time on the chloride diffusion of alkali-activated slag. Case Studies in Construction Materials 16 (2022) e00927. https://doi.org/10.1016/j.cscm.2022.e00927.

[118] Bondar D, Ma Q, Soutsos M, Basheer M, Provis JL, Nanukuttan S. Alkali activated slag concretes designed for a desired slump, strength and chloride diffusivity. Constr Build Mater 190 (2018) 191–199. https://doi.org/10.1016/j.conbuildmat.2018.09.124.

[119] Lee NK, Jang JG, Lee HK. Shrinkage characteristics of alkali-activated fly ash/slag paste and mortar at early ages. Cem Concr Compos 53 (2014) 239–248. https://doi.org/10.1016/j.cemconcomp.2014.07.007.

[120] Fan X, Wang Y, Yu Q, Gao X, Ye J, Zhang Y. Improving the chloride binding capacity of alkali activated slag by calcium and aluminum enriched minerals. Journal of Building Engineering 70 (2023) 106384. https://doi.org/10.1016/j.jobe.2023.106384.

[121] Zhang Y, Fang Y, Shen Y, Yang Z, Wu K. Chloride penetration and binding behavior in unsaturated alkali-activated slag mortars. Cem Concr Compos 140 (2023) 105098. https://doi.org/10.1016/j.cemconcomp. 2023.105098.

[122] Zhang J, Ma Y, Zhang Z, Yang Z, Nong X, Wang H. Effects of Mg-based admixtures on chloride diffusion in alkali-activated fly ash-slag mortars. Case Studies in Construction Materials 21 (2024) e03659. https://doi.org/10.1016/j.cscm.2024.e03659.

[123] Ye H, Huang L, Chen Z. Influence of activator composition on the chloride binding capacity of alkali-activated slag. Cem Concr Compos 104 (2019) 103368. https://doi.org/10.1016/j.cemconcomp.2019.103368.

[124] Ke X, Bernal SA, Provis JL. Uptake of chloride and carbonate by Mg-Al and Ca-Al layered double hydroxides in simulated pore solutions of alkali-activated slag cement. Cem Concr Res 100 (2017) 1–13. https://doi.org/10.1016/j.cemconres.2017.05.015.

[125] Ismail I, Bernal SA, Provis JL, San Nicolas R, Brice DG, Kilcullen AR, Hamdan S, Van Deventer JSJ. Influence of fly ash on the water and chloride permeability of alkali-activated slag mortars and concretes. Constr Build Mater 48 (2013) 1187–1201. https://doi.org/10.1016/j. conbuildmat.2013.07.106.

[126] Fan J, Zhu H, Shi J, Li Z, Yang S. Influence of slag content on the bond strength, chloride penetration resistance, and interface phase evolution of concrete repaired with alkali activated slag/fly ash. Constr Build Mater 263 (2020) 120639. https://doi.org/10.1016/j.co nbuildmat.2020.120639.

[127] Fang S, Lam ESS, Li B, Wu B. Effect of alkali contents, moduli and curing time on engineering properties of alkali activated slag. Constr Build Mater 249 (2020) 118799. https://doi.org/10.1016/j.conbuildm at.2020.118799.

[128] Provis JL, Myers RJ, White CE, Rose V, van Deventer JSJ. X-ray microtomography shows pore structure and tortuosity in alkali-activated binders. Cem Concr Res 42 (2012) 855–864. https://doi.org/10.1016/j.cem

conres.2012.03.004.

[129] Chi M. Effects of dosage of alkali-activated solution and curing conditions on the properties and durability of alkali-activated slag concrete. Constr Build Mater 35 (2012) 240–245. https://doi.org/10.1016/j.conbuildmat.2012.04.005.

[130] Chen X, He Y, Lu L, Wang F, Hu S. Effects of curing regimes on the chloride binding capacity of cementitious materials. Constr Build Mater 342 (2022) 127929. https://doi.org/10.1016/j.conbuildmat.2022.127929.

[131] ASTM C1202-19. Test Method for Electrical Indication of Concretes Ability to Resist Chloride Ion Penetration, (2019). https://doi.org/10.1520/C1202-19.

[132] Angulo-Ramírez DE, Valencia-Saavedra WG, Mejía de Gutiérrez R. Alkali-activated concretes based on fly ash and blast furnace slag: Compressive strength, water absorption and chloride permeability. Ingeniería e Investigación 40 (2020). https://doi.org/10.15446/ing.investig. v40n2.83893.

[133] Ampadu KO, Torii K, Kawamura M. Beneficial effect of fly ash on chloride diffusivity of hardened cement paste. Cem Concr Res 29 (1999) 585–590. https://doi.org/10.1016/S0008-8846(99)00047-2.

[134] Liu J, Wang X, Qiu Q, Ou G, Xing F. Understanding the effect of curing age on the chloride resistance of fly ash blended concrete by rapid chloride migration test. Mater Chem Phys 196 (2017) 315–323. https: //doi.org/10.1016/j.matchemphys.2017.05.011.

[135] Bondar D, Basheer M, Nanukuttan S. Suitability of alkali activated slag/fly ash (AA-GGBS/FA) concretes for chloride environments: Characterisation based on mix design and compliance testing, Constr Build Mater 216 (2019) 612–621. https://doi.org/10.1016/j.conbuildmat.2019.05.043.

[136] Zhang J, Ma Y, Zheng J, Hu J, Fu J, Zhang Z, Wang H. Chloride diffusion in alkali-activated fly ash/slag concretes: Role of slag content, water/binder ratio, alkali content and sand-aggregate ratio. Constr Build Mater 261 (2020) 119940. https://doi.org/10.1016/j.conbuildmat.2020.119940.

[137] Zhang J, Shi C, Zhang Z. Chloride binding of alkali-activated slag/fly ash cements. Constr Build Mater 226 (2019) 21–31. https://doi.org/10.1016/j.conbuildmat.2019.07.281.

[138] Babaee M, Castel A. Chloride diffusivity, chloride threshold, and corrosion initiation in reinforced alkali-activated mortars: Role of calcium, alkali, and silicate content. Cem Concr Res 111 (2018) 56–71. https://doi.org/10.1016/j.cemconres.2018.06.009.

[139] Wang X, Kong L, Zhao W, Liu Y. Chloride transport resistance of alkali-activated concrete exposed to combined chloride, sulfate and carbonation environment. Constr Build Mater 367 (2023) 130353. https://doi.org/10.1016/j.conbuildmat.2023.130353.